



UNIVERSITÀ DI PARMA

ARCHIVIO DELLA RICERCA

University of Parma Research Repository

A respirable HPV-L2 dry-powder vaccine with GLA as amphiphilic lubricant and immune-adjuvant

This is the peer reviewed version of the following article:

Original

A respirable HPV-L2 dry-powder vaccine with GLA as amphiphilic lubricant and immune-adjuvant / Rossi, I.; Spagnoli, G.; Buttini, F.; Sonvico, F.; Stellari, F.; Cavazzini, D.; Chen, Q.; Muller, M.; Bolchi, A.; Ottonello, S.; Bettini, R.. - In: JOURNAL OF CONTROLLED RELEASE. - ISSN 0168-3659. - 340:(2021), pp. 209-220. [10.1016/j.jconrel.2021.11.002]

Availability:

This version is available at: 11381/2905614 since: 2021-12-20T10:39:04Z

Publisher:

Elsevier B.V.

Published

DOI:10.1016/j.jconrel.2021.11.002

Terms of use:

Anyone can freely access the full text of works made available as "Open Access". Works made available

Publisher copyright

note finali coverpage

(Article begins on next page)

12 July 2024

Journal of Controlled Release

A respirable HPV-L2 dry-powder vaccine with GLA as amphiphilic lubricant and immune-adjuvant --Manuscript Draft--

Manuscript Number:	COREL-D-21-01015R1
Article Type:	Research paper
Keywords:	pulmonary vaccination; dry powder for inhalation; spray drying; human papillomavirus; glucopyranosyl lipid A
Corresponding Author:	Ruggero Bettini, PhD University of Parma: Universita degli Studi di Parma Parma, ITALY
First Author:	Irene Rossi
Order of Authors:	Irene Rossi Gloria Spagnoli Francesca Buttini Fabio Sonvico Fabio Stellari Davide Cavazzini Quigxin Chen Martin Müller Angelo Bolchi Simone Ottonello Ruggero Bettini, PhD
Abstract:	<p>Vaccines not requiring cold-chain storage/distribution and suitable for needle-free delivery are urgently needed. Pulmonary administration is one of the most promising non-parenteral routes for vaccine delivery. Through a multi-component excipient and spray-drying approach, we engineered highly respirable dry-powder vaccine particles containing a three-fold repeated peptide epitope derived from human papillomavirus (HPV16) minor capsid protein L2 displayed on <i>Pyrococcus furiosus</i> thioredoxin as antigen. A key feature of our engineering approach was the use of the amphiphilic endotoxin derivative glucopyranosyl lipid A (GLA) as both a coating agent enhancing particle de-aggregation and respirability as well as a built-in immune-adjuvant. Following an extensive characterization of the <i>in vitro</i> aerodynamic performance, lung deposition was verified <i>in vivo</i> by intratracheal administration in mice of a vaccine powder containing a fluorescently labeled derivative of the antigen. This was followed by a short-term immunization study that highlighted the ability of the GLA-adjuvanted vaccine powder to induce an anti-L2 systemic immune response comparable to that of the subcutaneously (s.c.) administered liquid-form vaccine. Despite the very short-term immunization conditions employed for a preliminary vaccination experiment, the intratracheally administered dry-powder, but not the s.c. injected liquid-state, vaccine induced consistent HPV neutralizing responses. Overall, the present data provide proof-of-concept validation of a new formulation design to produce of a dry-powder vaccine that may be easily transferred to other antigens.</p>



**UNIVERSITÀ
DI PARMA**

**DIPARTIMENTO DI SCIENZE
DEGLI ALIMENTI E DEL FARMACO**

Parma, September 14th, 2021

Prof. Dr. Christine Allen
Editor-in-Chief
Journal of Controlled Release

Dear Professor Allen,

enclosed, please find the revised version of our manuscript "**A respirable dry-powder vaccine containing GLA as an amphiphilic lubricant and immune-adjuvant: proof-of-concept testing with an inhalational human papillomavirus L2-based immunogen**" to be considered for publication in *Journal of Controlled Release*.

We carefully considered all the points raised by the Reviewers and modified the manuscript accordingly.

As also reported in the attached point-by-point reply to the Reviewers' comments, we are grateful to the Reviewers for the time they dedicated to our work and for the useful suggestions they provided. We have addressed all the points raised by the Reviewers and substantially improved the overall quality (and readability) of the manuscript.

As to the criticism of Reviewer n. 3 which, by the way, is in stark contrast with the overall positive judgments expressed by the other Reviewers, we are convinced that the key factor for successful vaccine production has been clearly stated at the end of the 'Introduction' section of our manuscript.

We also believe that our paper, which has a clearly spelled out rationale, reports a full characterization of an innovative formulation and a preliminary, yet quite extensive and convincing set of *in vivo* data on the distribution and immunogenicity of the PfTrx-HPV-L2-GLA powder vaccine.

I look forward to your kind reply.

Sincerely yours,

Ruggiero Bettini, Ph.D.
Professor of Pharmaceutical Technology and Drug Delivery
Food and Drug Department, University of Parma
Parco Area delle Scienze 27/A
43124 Parma, Italy
Tel. +39 0521 905089 e.mail bettini@unipr.it

Answer to Reviewers' comments

First of all, we would like to thank the Reviewers for the time they have dedicated to our work and for the useful suggestions. We have addressed the points raised by the Reviewers to improve the quality of the manuscript.

Below our answers (in red) to the Reviewers comments.

Reviewer #1: In this manuscript, Bettini and co-authors developed a method to achieve a respirable dry-powder vaccine not requiring cold-chain storage/distribution. First, authors validated the excipient (mannitol, lactose and trehalose) to prevent the protein aggregation and achieve a high production yields. Next, authors evaluated the immunogenicity of the intratracheally delivered dry-powder vaccine compared with s.c injected protein vaccine or reconstituted dry-powder vaccine. Intratracheally delivered dry-powder vaccine showed comparable immune response compared to controls. However, before the acceptance of the manuscript, there are several points that need to be addressed. Below are specific comments.

1. In the legend of figure 1, 0.83%, 1.33%, 2.00% represents different amounts of the antigen which is not coincide with the table 1.

Table 1 refers to a first set of antigen-lacking powders produced with different amounts of sodium stearate as a surfactant and a technological surrogate of the (highly expensive) amphiphilic immune-adjuvant monophosphoryl lipid A. Then we moved to the production of powders with 1% sodium stearate and different contents of antigen (Figure 1). We realize that the presentation of the different powder sets was not clear enough. Therefore, we added a Table in the Supplementary, (new Table S1), summarising the compositions of the various powder prepared and investigated. We also explained in the text the coding of the second set of powders.

2. In table 1, the production yield is quite low, so is there a purification step to remove the not-dry-powder proteins? If not, it is hard to tell if the immunogenicity is owing to the dry-powder protein. Please include description to explain this.

The ratio between the protein antigen and the bulking agent is very low and strongly favors the latter component (antigen= 2% w/w, mannitol nearly 98% w/w as reported in the new Table S1), so it is hard to imagine that even a small fraction of the protein was not incorporated into the powder. Also, the marked difference between the liquid and the dry-powder form of the vaccine we observed in immune responses measured by ELISA or PBNA could not be explained if a large fraction of the antigen were free, i.e., not entrapped into powder particles.

3. In figure 1, the size of the dry-powder vaccine is more than 1 μ m, which is quite large. What is the size of the original protein? Please include description to explain the size difference.

The size difference between the produced powders and the antigen molecules is at least two orders of magnitude. Powders have a size in the range of a few microns, while the protein antigen, which in SEC analysis elutes as a dimer, has an estimated hydrodynamic diameter (determined by DLS) of approximately 300 nm. We believe there is no need for any further explanation.

4. In figure 3, size of 2.00% w/w PfTrx-HPV-L2 is smaller than 1.33% w/w of PfTrx-HPV-L2. Please include description to explain the size difference between two.

Figure 3 reports images of powder samples selected to highlight the morphological features of the two powders rather than the size distribution. The difference between the median particle size of

the two powders was not statistically significant ($D_{v,50}$ of $2.39 \pm 0.24 \mu\text{m}$ for Powder #5 and $2.65 \pm 0.18 \mu\text{m}$ for Powder #6).

5. A bar graph or actual value description would be helpful to supply in Figure 4A and Figure 5A to summarize the fluorescence.

A reference false-color scale, from which the actual values can be extrapolated, was already included in Figure 4A.

A similar false-color scale has been added to the revised Fig 5 A.

Actual fluorescence values were also added to the revised Figures 4A and 5A.

6. In the legend of figure 6, there is no explanation on #1 group. Figure 6c and d are missing #1 group.

Thanks for pointing out this insufficient disclosure. Figure 6 legend has been modified to fix this information gap.

Reviewer #2: This manuscript investigates respirable vaccine dry-powder containing GLA as multifunctional additive. It has good rationale and shows meaningful scientific data. But it needs to check some point for the publication of JCR.

We are grateful for the positive evaluation of our work.

Main concern:

First of all, the main concern of this manuscript is that most are just explanations of the results and lack the discussion in result part. Especially, there is no direct data on lubricant function of GLA. This must be provided.

To highlight the lubricant functionality of GLA, we have added a paragraph reporting the flow data of a GLA-containing powder vs the one containing sodium stearate. A corresponding methodological paragraph has been added to the 'Methods' section as well.

Minor concern:

1. page 2: Abbreviation of PSD should be "particle size distribution". IVIS should be "In vivo Imaging System"

The typos have been corrected.

2. line 154: in order to avoid confusion, the Formulations should be explained using a Table to mention the components in detail.

Thanks for pointing out this insufficient disclosure. Indeed, the presentation of the different powder sets was not clear enough. Therefore, according to the Reviewer suggestion, we added a Table to the Supplementary material (presented as Table S1 in the revised ms.), summarising the various powders prepared and investigated. We also better explained in the text the coding of the second set of powders.

3. line 156: Balking agent -> bulking agent???

The typo has been corrected.

4. line 165: Outlet temperature should be described as a dependent value.

We definitively agree with the point raised by the Reviewer. The outlet temperature is a dependent parameter that changes with several factors including equipment geometry, formulation composition, feed rate, drying air humidity and ambient temperature. That is why we usually do not

report this parameter because we believe it is of little, if any, usefulness for the purposes of reproducibility of the spray-drying process.

3. line 205: it needs to define about fine particle fraction with cut-off diameter of stages. FPF% refers to the percentage deposited on a stage that is typically less than 5 m. How did the author calculate it? The ACI result should be displayed for cut-off diameter of stages and the FPF% calculation equation should be attached. The FPF% cut-off diameter must be clearly stated. It also needs to explain why a glass microfiber filter was used without using a coating method.

We have added the cut-offs-diameters of the stages as they have been calculated according to the USP, plus a sentence to better explain how the FPD was calculated.

4. line 315: It would be better if it mentioned with exact number how much vaccine powder emitted from the insufflator in test group.

We added this information in the Methods.

5. line 393: It is difficult to mention mannitol as the best bulking agent "the superior production yields it afforded and the superior aerodynamic performance of the protein-containing powder" just based on Yield (%), EF (%) and RF (%). it was just prepared by one condition without consideration of particle properties.

We added a sentence to clarify that the above statement should not be taken in absolute terms but rather referred to the specific conditions that have been tested.

6. line 400: in Table1, what is the reason of the low yield of Powder #2 compared to other formulations? What is the size distribution?

That was a mistake. We apologize and thank the Reviewer for having pointed it out. The actual value is 31.53. We corrected the value in Table 1. It is still the lowest one, but not so different from the other values and falls within the typical range of yields for powders produced with this type of equipment.

7. line 435: Figure 2 (A) What is the migration artifact? It is appeared that the molecular weight in changed by spray drying process. No y axis title for Fig 2b.

What we meant by 'migration artifact' is the so-called 'smile effect', that is a difference in apparent electrophoretic mobility between samples loaded into a right-most lane (in this case DP) and an inner lane (in this case UT). Indeed, as shown by the results of a similar electrophoretic analysis presented in panel 3C, there is no appreciable difference in the apparent molecular weights of the untreated and spray-dried PfTrx-HPV-L2 antigen. However, to avoid any possible misunderstanding, we removed from Figure 2 legend the sentence referring to a migration artefact and this slight difference in electrophoretic mobility.

A y-axis descriptor has been added to the revised Figure 2B.

8. line 459-461: this sentence to explain that it prepared same molecular concentration 1% fractional amount of sodium stearate. For this that it should be prepared 5.75% GLA not 0.17%?? Please confirm them.

We added a sentence to better explain this point. We assumed that a lower amount of a larger molecule is needed to cover the same surface, thus the GLA concentration was scaled down according to the ratio 306.5/1763.5, which turns out to be approximately 0.17.

9. line 486: The SEM images of prepared particle showed broad particle size and the magnified SEM images (X20K) showed the most of particle are under 1 micron. It needs to explain with span value or Dv10 or Dv90 values. No y-axis title for Fig 3d.

The requested values have been added to the revised manuscript.

A y-axis descriptor has been added to the revised Figure 3D.

10. line 492: please insert "mean \pm SD"

As specified at the end of the Methods section (line 371 of the original manuscript), unless otherwise indicated, all values are expressed as the mean \pm standard deviation. So, we think it is not really essential to repeat this specification throughout the text.

11. line 492: What is the reason to choose Powder #6 final formulation? Please explain.

We added a sentence to explain that powder #6 was selected as it was the one containing the highest amount of antigen.

12. line 501: please insert the Standard deviation

Done.

13. line 505-509: please mention concrete numbers, and it should be noted if there is a statistical difference. For this discussion, specific experimental data for moisture reduction should confirmed such as Karl Fischer or surface charge depletion.

We deleted the sentence dealing with water loss or charge dissipation as potential explanations of the observed effect because the differences between EF and FPM, before and after storage, turned out not to be statistically significant.

14. line 532: Fig4A/4B lacks the legibility of the figure. Fig4C: What is the value? (Average?) If the value is average, the intensity legend is not matched with values and images.

Figure 4A presents the results of total fluorescence signal quantification within the thorax region that is enclosed by the white cube shown in the background. Figure 4B shows the results of Micro-CT imaging. False-color scales and the actual fluorescence intensity values measured in those areas are now reported in the revised Figure 4.

Figure 4C (whole mouse image) is just a representative epifluorescence picture obtained with the IVIS instrument and as such it is not quantifiable in a precise manner.

Lung, liver, kidneys and spleen fluorescence data were obtained by *ex-vivo* imaging and the amount/intensity of fluorescence in each district was quantified and expressed as a total fluorescence signal normalized per second and surface area (cm²).

15. line 591: The Group # No. and Formulation # No can be confused. Please confirm that.

We added the word Group before # to resolve this ambiguity and avoid any possible confusion.

16. line 596: There is no explanation for group #4

Group #4 was actually described at the very beginning of this paragraph (line 592), but for the sake of clarity and in response to the Reviewer's point, in the revised manuscript it is now described sequentially, together with the other groups, at the end of the paragraph.

17. line 600: Fig 6B is not shown the standard deviation.

Since the results in Figure 6B are presented as single-animal data-points, there is actually no reason for providing a standard deviation value.

In Fig6D, Whether HPV16 neutralization titers were evaluated using the same sample as the GST-L2 ELISA. Why the number of samples is different?

As specified in the revised legend to Figure 6D, only a subset of the sera analyzed by GST-L2-ELISA (Figure 6B) were actually assayed for virus neutralization capacity using the L2-PBNA. Leaving out the sera from the negative control group (#1), which were found to be completely devoid of HPV16-L2 reactive antibodies, for the determination of neutralizing antibody titers with the L2-PBNA, we focused on a subset of five immune-sera/group (groups #2, #3 and #4) derived from the animals in each group that displayed the highest (top five) anti-HPV-L2 total antibody titers by GST-L2 ELISA (Figure 6B).

Reviewer #3: The authors developed an antigen powder formulation for the respirable vaccine. As a component to stabilize it, the an adjuvant GLA was used. The authors reported on the physicochemical property, tissue distribution and its antigen-producing activity.

Overall, it is not clear what is a key factor for the successful antigen production. The authors developed a 4 set of formulation (Table 1). However, the tissue distribution, intra-lung distribution was systemically analyzed. I think the manuscript is too preliminary to be accepted in JCR. The other comments are listed below:

We disagree with the Reviewer's criticism, which contrasts with the overall positive judgments expressed by the other Reviewers. In our humble opinion, the key factor for successful vaccine production has been clearly stated at the end of the Introduction (lines 109-117 in the original manuscript).

In fact, we are convinced that our paper, which has a clearly explained rationale, reports a full characterisation of an innovative formulation and a preliminary, yet quite extensive and convincing set of *in vivo* data on the distribution and immunogenicity of the PfTrx-HPV-L2-GLA powder vaccine.

1. It is not clear how the authors optimized their system. Especially, what is a key parameter for the optimization.

As explained in the manuscript (lines 426-428), the optimization was based on process yield and powder respirability.

2. In table 1, the authors developed 4 set of formulation. In this case, the content of sodium stearate was varied. In this formulation the amount of GLA is same?

These formulations did not contain GLA. As stated in the manuscript, sodium stearate was used in preliminary set-up experiments as a surfactant and a technological surrogate of the amphiphilic immune-adjuvant glucopyranosyl lipid A. However, we realize that the presentation of the different powder sets was not clear enough, and we thank the Reviewer for underlining the point. Therefore, we added a Table in the Supplementary, summarising the various powder prepared and investigated. We have also explained in the text the coding of the second set of powders.

3. The authors reported that the antigen is distributed to the liver. I worry that the activated immune-system attack the antigen presenting cells in liver. The toxicity, especially in repeated injection must be analyzed.

As mentioned in section 3.3 (lines 547-563) a fairly strong *in-vivo* fluorescence signal was indeed observed in the liver. Importantly, however, subsequent *ex-vivo* analyses, most notably SDS-PAGE fractionation coupled to Alexa-based near-infrared antigen visualization, clearly revealed the

absence of any detectable, protein antigen-associated fluorescence signal in the case of liver extracts. In our opinion (see lines 562-564), this indicates that Alexa labelled peptide fragments, rather than the intact PfTrx-HPV-L2 antigen, were actually transferred to the liver, probably on the way toward further degradation and, ultimately, elimination. Based on this result, we do not see any risk of 'activated immune-system attack of antigen presenting cells in the liver', nor long-term toxicity of our respiratory tract-delivered dry-powder vaccine.

4. In Fig 6, the antibody production in #4 seems to be highest. What is a mechanism?

Since total anti-HPV16-L2 antibody titers measured in the three groups (#2, 3, 4) by ELISA (panel 6B) are quite similar, we suppose that the Reviewer is actually referring to the data presented in panel 6D. These are the results of pseudovirion-based neutralization assays (PBNA), which specifically measure neutralizing (not total) anti-L2 antibodies, i.e., antibodies that are capable to prevent virus entry into engineered target cells. As pointed out by the Reviewer, the production of these particular (virus-neutralizing) antibodies seems to be highest in group #4, which is composed of mice that were immunized with the intratracheally delivered dry-powder PfTrx-HPV-L2 vaccine. The actual reasons for this apparent superiority are presently unknown. However, given the short immunization schedule utilized for our preliminary immunogenicity assessment, as briefly mentioned at the end of section 3.4 (lines 643-646), we speculate that this might reflect a faster affinity-maturation of anti-HPV-L2 antibodies and a more effective production of virus-neutralizing antibodies.

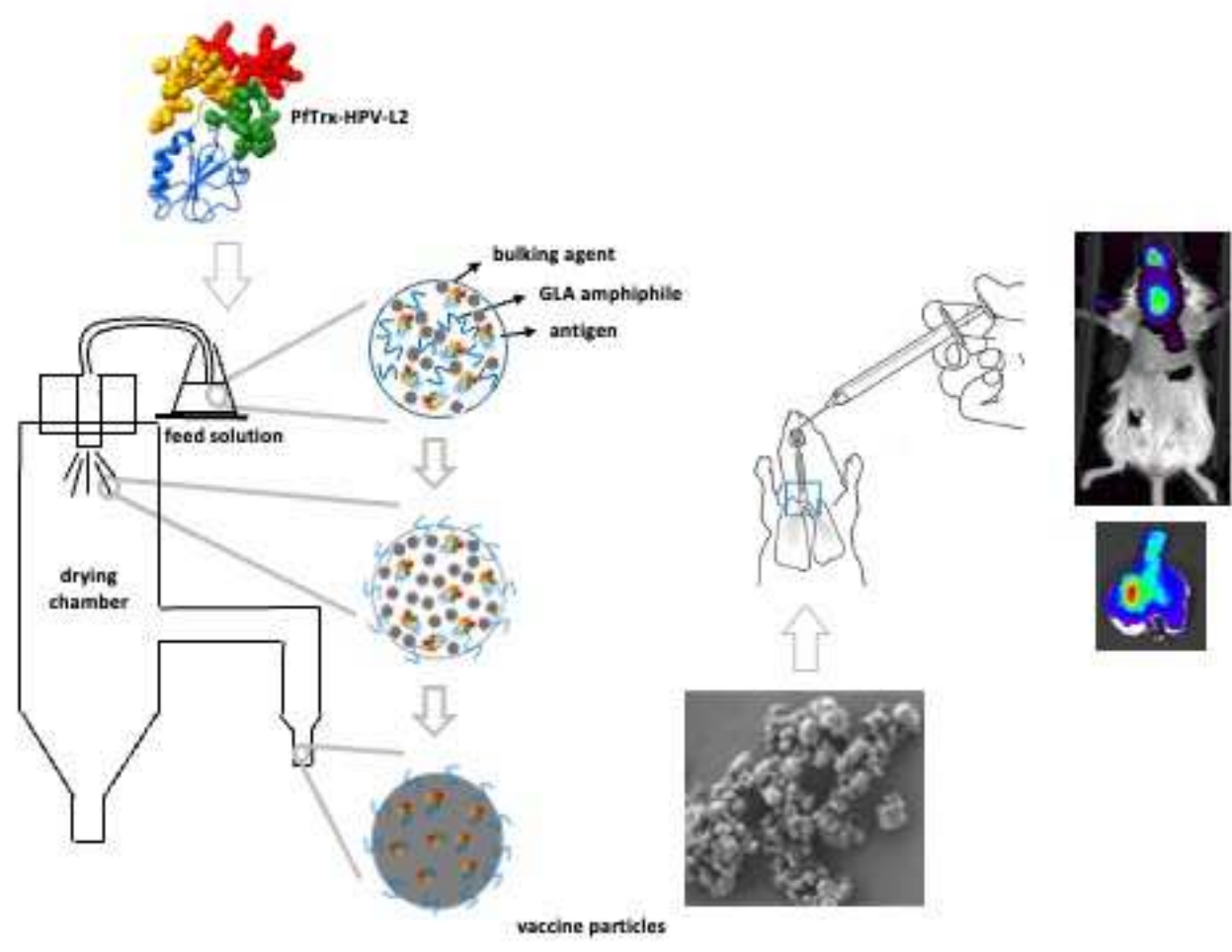
5. In relation to the comment 4, the antigen production appeared in all-or-none pattern. Why?

This comment, that, we suppose, again refers to the L2-PBNA data in Figure 6D, is not entirely correct. In fact, although the best responses (especially with regard to the number of responding animals) were measured in group #4 (intratracheally delivered dry-powder PfTrx-HPV-L2 vaccine), a good response was also observed for group #3 (PfTrx-HPV-L2-GLA powder, dissolved in PBS prior to subcutaneous injection). It would be tempting to speculate that the antigen+GLA formulation *per se* (i.e., even after solubilization and subcutaneous injection), in addition to intratracheal delivery of the dry-powder vaccine, somehow also positively influences neutralizing antibody production, but the data we have collected so far are not sufficient to support this hypothesis. To further clarify the conceptual difference between the data reported in Figure 6B and 6D, specific y-axis descriptors have been added to both figures.

Reviewer #4: Vaccines not requiring cold-chain storage/distribution and suitable for needle-free delivery are urgently needed. Pulmonary administration is one of the most promising non-parenteral routes for vaccine delivery.

The aim of this study to develop and test a dry-powder inhalatory (DPI) formulation of a HPV vaccine based on a previously described L2 antigen, in which three copies of the HPV16 L2 major cross-neutralization epitope comprised between amino acids 20-38 are grafted intramolecularly to *Pyrococcus furiosus* thioredoxin (hereafter designated as PfTrx-HPV-L2). The PfTrx-HPV-L2 DPI vaccine was produced by spray-drying through a particle engineering approach based on the molecular deposition of an amphiphilic immune-adjuvant (glucopyranosyl lipid A; GLA) on the surface of the spray-dried particles. It is an interesting and well designed study.

We are grateful to the Reviewer for her/his nice comments and extremely honoured for her/his great consideration of our work.



A respirable HPV-L2 dry-powder vaccine with GLA as amphiphilic lubricant and immune-adjuvant

Formatted: Centered

A respirable dry-powder vaccine containing GLA as an amphiphilic lubricant and immune-adjuvant: proof-of-concept testing with an inhalational human papillomavirus L2-based immunogen

Formatted: Centered

Irene Rossi^{1,3,§^}, Gloria Spagnoli^{2,3§}, Francesca Buttini^{1,3}, Fabio Sonvico^{1,3}, Fabio Stellari⁴, Davide Cavazzini², Quixin Chen⁵, Martin Müller⁵, Angelo Bolchi^{2,3}, Simone Ottonello^{2,3*}, Ruggero Bettini^{1,3*}

¹Department of Food and Drug Sciences, ²Department of Chemistry, Life Sciences and Environmental Sustainability, and ³Interdepartmental Center Biopharmanet-tec, University of Parma, Parco Area delle Scienze Parma, Italy.

⁴Chiesi Farmaceutici SpA, Largo Belloli 11a, Parma, Italy.

⁵German Cancer Research Center, Im Neuenheimer Feld 280, Heidelberg, Germany.

[^] Present address: Nanopharm Ltd, An Aptar Pharma Company, Newport, United Kingdom.

[§]Equally contributing to the paper.

*Corresponding authors:

Ruggero Bettini

Parco Area delle Scienze 27/A, 43124 Parma, Italy

e.mail: ruggero.bettini@unipr.it

Phone: * 39 0521 905089

Field Code Changed

Simone Ottonello

Parco Area delle Scienze 11/A, 43124 Parma, Italy

e.mail: simone.ottonello@unipr.it

Phone: +39 0521 905646

Field Code Changed

Abbreviations

GLA= Glucopyranosyl Lipid A

MPLA= Monophosphoryl Lipid A

HPV16= Human Papillomavirus

S.C.= Subcutaneous

I.T.= Intratracheal

DPI= Dry Powder Inhaler

EM= Emitted Mass

EF= Emitted Fraction

RM= Respirable Mass

RF= Respirable Fraction

MMAD= Mass Median Aerodynamic Diameter

GSD= Geometrical Standard Deviation

FSI= Fast Screening Impactor

ACI= Andersen Cascade Impactor

PSD= Particle Size Distribution

SEM= Scanning Electron Microscopy

DVS= Dynamic Vapor Sorption

TGA= Thermogravimetric Analysis

ELISA= Enzyme-Linked Immunosorbent Assay

SDS-PAGE= Sodium Dodecyl Sulphate Polyacrylamide Gels

Micro-CT= Micro-Computed Tomography

IVIS= *In vivo* Imaging System

1 **Abstract**

2 Vaccines not requiring cold-chain storage/distribution and suitable for needle-free delivery are
3 urgently needed. Pulmonary administration is one of the most promising non-parenteral routes for
4 vaccine delivery. Through a multi-component excipient and spray-drying approach, we engineered
5 highly respirable dry-powder vaccine particles containing a three-fold repeated peptide epitope
6 derived from human papillomavirus (HPV16) minor capsid protein L2 displayed on *Pyrococcus*
7 *furiosus* thioredoxin as antigen. A key feature of our engineering approach was the use of the
8 amphiphilic endotoxin derivative glucopyranosyl lipid A (GLA) as both a coating agent enhancing
9 particle de-aggregation and respirability as well as a built-in immune-adjuvant. Following an
10 extensive characterization of the *in vitro* aerodynamic performance, lung deposition was verified *in*
11 *vivo* by intratracheal administration in mice of a vaccine powder containing a fluorescently labeled
12 derivative of the antigen. This was followed by a short-term immunization study that highlighted
13 the ability of the GLA-adjuvanted vaccine powder to induce an anti-L2 systemic immune response
14 comparable to that of the subcutaneously (s.c.) administered liquid-form vaccine. Despite the very
15 short-term immunization conditions employed for a preliminary vaccination experiment, the
16 intratracheally administered dry-powder, but not the s.c. injected liquid-state, vaccine induced
17 consistent HPV neutralizing responses. Overall, the present data provide proof-of-concept
18 validation of a new formulation design ~~for the production of to produce~~ a dry-powder vaccine that
19 may be easily transferred to other antigens.
20

21

22 **Key words:** pulmonary vaccination, dry powder for inhalation, spray drying, human papillomavirus,
23 glucopyranosyl lipid A.
24

25

26 **1. Introduction**

27 Vaccination is an established cost-effective strategy for the prevention of infectious (and some non-
28 infectious) diseases [1,2] and its value as a life-saving tool is all the more appreciated during the
29 present SARS-CoV2 pandemics [3]. Regardless of their attenuated/inactivated whole virus or
30 recombinant nature, most present-day vaccines require a strict cold-chain maintenance ~~in-order~~
31 ~~to~~ remain active. Indeed, cold-chain maintenance accounts for approximately 50% of vaccine cost
32 on average and a similar fraction of the total vaccine production is thought to be wasted or damaged
33 due to cold-chain breakage [4,5]. This is both an economical and a healthcare problem, which
34 especially (but not exclusively) impacts on low-and-middle-income countries (LMICs), that is the
35 very places where vaccination is most needed. An additional drawback associated to most current
36 vaccines is that they are commonly administered via intramuscular (i.m.) or subcutaneous (s.c.)
37 injection. This mode of delivery requires trained medical personnel, may face religious and/or
38 ethnical barriers, and comes with the inherent risk, especially in LMICs, of needle-stick related
39 injuries and potential infections. Even in high-income countries, adverse reactions to parenteral,
40 needle-requiring vaccine administration (so-called 'lipothymic reaction' or 'needle-phobia') [6] as
41 well as the burden of this mode of administration on the healthcare system have been documented.
42 Novel vaccine formulations, compatible with viral and protein-based subunit antigens, suitable for
43 non-parenteral administration are thus actively sought as a possible solution to the ~~above~~
44 ~~describedabove-described~~ limitations of current vaccines. Solid-dosage vaccines (i.e., lyophilized or
45 powder form vaccines) are reportedly more stable than their corresponding liquid forms, both from
46 the biochemical (i.e., antigen structural integrity) and microbiological point of view, due to the
47 absence of water [7]. This makes them amenable to non-cold-chain distribution and a more
48 extensive stockpiling. However, due to the general sensitivity of proteins to dehydration, water
49 removal is a risky step for the maintenance of antigen integrity. These potentially adverse effects
50 can be suppressed, or at least minimized, by the addition of sugars (e.g. trehalose), polyols (e.g.
51 mannitol), polysaccharides (e.g. dextran) or amino acids (e.g. L-leucine) as stabilizing agents and
52 antigen-protective excipients [8-14].

53 Among the various routes of non-parenteral vaccine administration, pulmonary vaccination is
54 gaining momentum due to ~~a number of several~~ favorable features. These include the large surface
55 area, extended vascularization and abundance of dendritic cells and macrophages for antigen
56 capture of the respiratory tract, without exposure to a harsh environment such as the one found in
57 the gastro-intestinal tract. This, coupled with direct antigen delivery to a mucosal site, may result in
58 a more effective mucosal immunity without any interference with systemic immunity, thus allowing
59 for a broad application of this mode of immunization. An additional advantage of pulmonary
60 vaccination is its needle-free administration -a mode of delivery that in humans is facilitated by the
61 availability of well-developed dry powder inhalers [14].

62 The first attempts at pulmonary vaccination date back to the late 60's. These were based on the
63 inhalatory administration of either very low amounts of living attenuated *Mycobacterium bovis* [15]
64 or a liquid-form of aerosolized influenza vaccine [16], both of which led to successful immunization
65 and protection. Despite these promising initial results, follow-up studies on pulmonary vaccination
66 were discontinued, likely due to the lack of easy-to-use administration devices. They were resumed

67 more than 35 years later and extended to non-airborne infections such as hepatitis B (HBV),
68 diphtheria and measles (see #7 for a review). HBV and influenza have been the predominant test-
69 bench of pulmonary vaccination, and different types of variously adjuvanted immunogens, relying
70 on inactivated whole-virus but also on recombinant antigens, formulated by spray-freeze-drying and
71 delivered in either a liquid or a powder form have been investigated in different preclinical settings
72 for their lung deposition and immunogenicity [7,17,18].

73 In addition to the specific types of antigen and immune-adjuvant, the physical state of the vaccine
74 as well as its formulation and manufacturing, have also been shown to strongly influence the
75 immune performance of inhalatory vaccines [10,17,19-22]. Of note, powder vaccine formulations
76 have generally been found to be comparable, or superior, to liquid antigen formulations with regard
77 to immunogenicity, but with the added benefits of long-term stability and ease of delivery
78 [7,10,17,18,20-22]. Particle size and shape, and particularly an aerodynamic diameter smaller than
79 5 µm, are key features for achieving a suitable lung deposition [17-19]. Among the different drying
80 processes used ~~for the production of~~ to produce respirable particles, spray-drying stands up as the
81 most easily scalable procedure. Also, the aerodynamic performance of spray-dried powders has
82 been shown to be significantly improved by a particle engineering approach involving the addition
83 of small amounts of surfactant or amphiphilic molecules with lubricant functionality [23,24].

84 Similar to most licensed vaccines, current human papillomavirus (HPV) vaccines, which rely on
85 different combinations of major capsid protein L1 virus-like particles (VLP) [25], also have to be
86 continuously refrigerated during storage/distribution [26]. Following-up to the encouraging results
87 obtained with liquid-state, monotypic (HPV16) VLPs delivered through the airways via nasal
88 nebulization or bronchial aerosolization [27], two different dry-powder HPV vaccine formulations
89 were developed and tested for thermal stability and immunogenicity upon i.m. injection [28-30].
90 These powder vaccine formulations were produced by either a multicomponent excipient, spray-
91 dry system [28,29], or with the use of glass forming polymers and trehalose as spray-drying
92 excipients followed by atomic layer deposition to coat the resulting particles with defined layers of
93 the alum adjuvant [30]. Except for one study dealing with the thermal stability of a spray-dried
94 formulation of the nonavalent, Gardasil® 9 HPV vaccine [28], the other studies were focused on
95 simplified, intrinsically more thermostable HPV antigens, such as L1 capsomeres [30] and a peptide
96 epitope from minor capsid protein L2 incorporated into MS2 bacteriophage VLPs [29]. A substantial
97 increase in thermal stability along with an immunogenicity comparable to, or even higher than, that
98 of liquid vaccine controls was observed for both spray-dried and alum-coated vaccine formulations.
99 However, the resulting vaccine powders were always dissolved prior to immunization, which was
100 only performed by intramuscular injection, thus obviously precluding any information on dry-
101 powder vaccine respirability, lung deposition and immunogenicity upon pulmonary delivery.

102 To begin to fill these gaps, we developed and tested a dry-powder inhalatory (DPI) formulation of a
103 HPV vaccine based on a previously described L2 antigen [31,32], in which three copies of the HPV16
104 L2 major cross-neutralization epitope comprised between amino acids 20-38 are grafted
105 intramolecularly to *Pyrococcus furiosus* thioredoxin (hereafter designated as PfTrx-HPV-L2). The
106 thermal stability and immunogenicity of this particular antigen [31,32] as well as the preclinical
107 efficacy and cross-neutralization capacity of other antigens based on a similar L2 epitope [33] have
108 been documented previously.

Formatted: Font: Italic

109 The *PfTrx*-HPV-L2 DPI vaccine was produced by spray-drying through a particle engineering
110 approach based on the molecular deposition of an amphiphilic immune-adjuvant (glucopyranosyl
111 lipid A; GLA) on the surface of the spray-dried particles. The rationale behind this approach was to
112 improve both particle respirability as well as surface exposure of the adjuvant and its recognition by
113 lung immune cells, especially antigen presenting cells such as dendritic cells and macrophages [18].
114 The dry powder vaccine thus produced was extensively characterized with respect to aerodynamic
115 properties, including the assessment of its *in vivo* lung deposition capacity. The systemic
116 immunogenicity of the intratracheally delivered *PfTrx*-HPV-L2 DPI vaccine was also preliminarily
117 evaluated in a short-term immunization study in mice.

Formatted: Font: Italic

Formatted: Font: Italic

118

119

120 2. Materials and Methods

121

122 2.1 Materials

123 Mannitol, Pearlitol® SD 200 batch no. E556G, was a kind gift by Roquette Freres. Sodium stearate
124 was purchased from Magnesia GmbH. Glycopyranoside Lipid A (GLA, PHAD), synthetic version of
125 Monophosphoryl Lipid A (MPLA), was supplied by Avanti Polar Lipids. All solvents were at analytical
126 grade and ultrapure water (0.055 µS/cm, TOC 1 ppb) was produced by reverse osmosis (Purelab
127 Pulse + Flex ultrapure water, Elga-Veolia).

128

129 2.2 Methods

130 **2.2.1 PfTrx-HPV-L2 and GST-L2 constructs.** Codon-usage optimized *Pyrococcus furiosus* (*Pf*) Trx
131 (*PfTrx*) coding sequences were chemically synthesized (Eurofins MWG Operon) and inserted into
132 the *NdeI* site of a His-tag-lacking pET26 plasmid. Three tandemly repeated copies of the HPV16 L2
133 aa 20-38 peptide grafted to the display site of *PfTrx* was generated by inserting the corresponding
134 sequences into the Trx *CpoI* sites of pre-assembled pET-*PfTrx* plasmids as described previously
135 [31,32,34]. The resulting constructs were sequence-verified and transformed into *Escherichia coli*
136 BL21 codon plus (DE3) cells for recombinant protein expression.

137 Glutathione S-transferase (GST)-L2 fusion to be used as capture antigen for ELISA was produced by
138 cloning the L2 (aa 1-120) coding sequence into the *SmaI* site of the GST expression vector pGEX-4T-
139 2.

140

141 **2.2.2 Expression and purification of the PfTrx-HPV-L2 antigen.** Recombinant *PfTrx*-HPV-L2 was
142 produced by overnight induction at 30°C in auto-inducer medium (10 g/L yeast extract, 25 mM
143 NH₄SO₄, 50mM KH₂PO₄, 50 mM Na₂HPO₄, 2 mM glucose, 6 mM α-lactose, 1.2 mM MgSO₄). Following
144 cell lysis, the untagged *PfTrx*-HPV-L2 protein was purified by cation exchange chromatography and
145 detoxified by a three-fold repeated Triton X-114 (1% v/v) treatment [35]. Endotoxin (LPS) removal,
146 to levels lower than 2 EU/mL, was verified for each antigen batch by the LAL QLC-1000 test (Lonza).
147 The GST-L2 protein was affinity-purified on glutathione-sepharose columns (GE Healthcare)
148 according to the manufacturer's instructions. The composition and purity of individual protein
149 preparations were assessed by electrophoretic analysis on 11-15% SDS-polyacrylamide gels (SDS-
150 PAGE). Protein concentration was determined by measurement of absorbance at 280 nm using
151 calculated extinction coefficients [36] and with the use of a QubitH 2.0 Fluorometer (Life
152 Technologies).

153

154 **2.2.3 Spray drying.** Dried engineered powders for inhalation containing the antigen were produced
155 by spray drying with a mini Spray Dryer Büchi B-290 (Büchi Laboratoriums-Technik) in aspiration and
156 open mode. The feed solution was prepared by dissolving the bulking agent in ultrapure water
157 whereas the amphiphilic compound was dissolved in ethanol (95% v/v). The protein solution in 25
158 mM potassium phosphate buffer (pH 7.4) was, then, added to the water portion and ethanol
159 solution was added drop wise to the aqueous one under continuous magnetic stirring at 200 rpm

160 ~~order-to-to~~ reach a final solution with water to ethanol ratio 70:30 v/v. The total concentration of
161 solutes was always kept at 0.6% w/v.

162 The concentration of the bulking agent in the solution was adjusted for each formulation to
163 complement 0.6% w/v of the total solute taking into consideration the concentration of the protein
164 and the amphiphilic compound. [Formulations of the main powder tested are summarized in Table
165 S1 in Supplementary](#). The drying parameters were set as follow: inlet temperature, 125 °C; drying
166 air flow rate, 601 L/h; aspiration, 35 m³/h; solution feed rate, 3.5 mL/min and nozzle diameter, 0.7
167 mm.

168
169 **2.2.4 Particle size distribution by laser diffraction.** The particle size distribution (PSD) of spray dried
170 powders was measured by laser light scattering (Spraytec[®], Malvern Instruments Ltd). The
171 diffractometer was equipped with a 300 mm focal lens, which measures particle size in the range
172 0.1-900 µm. Samples were prepared by suspending 10 mg of powders in 10 mL of cyclohexane
173 containing 0.1% w/v of Span 85 (Honeywell Fluka[™]). To improve homogeneity, the dispersion was
174 put in an ultrasonic bath (8510, Branson Ultrasonics Corporation,) for 5 minutes before PSD
175 measurements that were carried out in triplicate for each sample with an obscuration threshold of
176 at least 10%. Data were expressed as volume diameter of 10th (D_{v,10}), 50th (D_{v,50}) and 90th (D_{v,90})
177 percentile of the particle population and as Span value $[(D_{v,90}-D_{v,10})/D_{v,50}]$.

178
179 **2.2.5 Scanning electron microscopy and powder flow.** A Scanning Electron Microscope (FESEM-FIB
180 Zeiss Auriga Compact, Carl Zeiss) was used to investigate particle morphology, shape and surface
181 characteristics of the spray dried powders. Powders were deposited on adhesive black carbon tabs
182 pre-mounted on aluminum stubs; powder in excess was removed with a gentle nitrogen flow, and
183 samples imaged without any metallization process. The microscope was operated after 30 min of
184 depressurization (1.87 10⁻⁴ Pa) with an accelerating voltage of 1.0 kV and a working distance of 4.9
185 mm. Images were taken at different magnification.

186 [Dynamic angle of repose was determined as an indicator of the powder flow properties.
187 Measurements were carried out according to Ph. Eur. 10th ed. employing a Friability tester \(model
188 TA3R, Erweka GmbH\) where the drum had been removed and replaced with a transparent glass vial
189 \(volume 10 mL\) filled with about 50 mg of powder. The vial was, then, attached to the tester arm
190 and rotated for 60 seconds at 20 rpm. A video was recorded with an iPhone 6 \(Apple\), and single
191 frames were extracted and analyzed with the software Image J64 \(NIH\) to measure the angle
192 between the horizontal lane and the powder avalanche line during the so-called rolling stage. Six
193 independent measurements were performed each tested powder.](#)

194
195
196 **2.2.6 In vitro aerodynamic performance assessment.** The aerodynamic performance of the
197 powders was firstly investigated using a Fast Screening Impactor, FSI, (Copley scientific Ltd.). 10 mg
198 of powder were loaded manually in a hypromellose Quali-V-I capsule size 3 (Qualicaps) and one
199 single capsule for each test was aerosolized using a high resistance RS01[®] device (RPC, Plastiapae,
200 [Osnaago, Italy](#)). The entire system was connected to a vacuum pump (Mod. 1000, Erweka GmbH,) which
201 created the air flow to aerosolize and distribute the powder in the FSI. The flow rate used

202 during each test was adjusted, according to current USP monograph, with a Critical Flow Controller
203 TPK (Copley Scientific Ltd) in order to produce a pressure drop of 4 kPa over the inhaler. Thus, flow
204 rate was set at 60 L/min before each experiment using a Flow Meter DFM 2000 (Copley Scientific
205 Ltd). The pump was activated for 4 seconds for each test so that to withdraw a volume of 4 L of air
206 from the inhaler. The aerosolization performance was tested in triplicate. The following parameters
207 were calculated: the emitted mass (EM) was the amount of powder that was emitted from the
208 device; the emitted fraction (EF) was calculated as the ratio between the EM and the amount of
209 powder loaded in the capsule. The respirable mass (RM) was the mass of powder with aerodynamic
210 diameter lower than 5 μm , ~~i.e.~~, the amount deposited on the filter (type A/E, diameter 76 mm,
211 Pall Corporation) of the Fine Fraction Collector (FFC); the respirable mass (RF) was calculated as the
212 ratio between RM and the amount of powder loaded in the capsule. EM and RM were calculated
213 from the weight of the device loaded with the filled capsule and the filter before and after the
214 aerosolization of the powder.

215 Andersen Cascade Impactor (ACI, Apparatus 3, USP 41, Copley scientific Ltd) was employed to
216 determine the aerodynamic distribution of the powder produced for the *in vivo* study. [The](#)
217 [measurements were carried out according to USP-NF <601>; thus, at the flow rate of 60 L/min \(see](#)
218 [below\), the cut-offs diameters of the stages -1, -0, 1, 2, 3, 4, 5, 6 were the following: 8.60, 6.50, 4.40,](#)
219 [3.20, 1.90, 1.20, 0.55 and 0.26 \$\mu\text{m}\$.](#) A glass microfiber filter of diameter 82.6 mm (Whatman plc,
220 [Little Chalfont, UK](#)) was placed right below stage six ~~in order~~ to collect particles with a diameter
221 lower than that ~~of the stage 6 cut-off~~ 0.26 μm . 20 mg of each powder were loaded in Quali-V-I size
222 3 capsules and the RS01[®] device was again employed for the aerosolization. Before running the
223 experiment, 2 mL of a solution of Tween[®] 1% w/v in ethanol was applied on the particle collection
224 surface of each stage; after complete solvent evaporation a thin layer of surfactant was obtained on
225 the stage surfaces that ensured efficient particle capture avoiding particle bouncing. An air flow rate
226 of was set at 60 L/min, (Flow Meter DFM 2000) was generated by a vacuum pump (SCP5, Copley
227 scientific Ltd) activated for 4 seconds, using the TPK to adjust the flow. After the powder
228 aerosolization, the powder deposited in the device was cumulated with that remained in the capsule
229 and collected in with ultrapure water in a 50 mL volumetric flasks; similar collection was done for
230 the powder deposited in the induction port. The powders deposited onto stages -1, -0 and 1 were
231 solubilized individually with 25 mL of ultrapure water, while for all the other stages 10 mL were
232 used. The filter was removed from the system and put in a crystallizer with 10 mL of ultrapure water
233 and put 5 minutes in an ultrasonic bath. The solutions obtained from the filter as well as that from
234 device plus capsule were filtered through a 0.45 μm cellulose acetate syringe filters (Labservice
235 Analytica), before injection in HPLC for the quantification of mannitol that was taken as tracer of
236 the particles. [Starting at the final collection site \(filter\), the cumulative mass versus cut-off diameter](#)
237 [of the respective stage was derived. The mass of mannitol with an aerodynamic diameter less than](#)
238 [5 \$\mu\text{m}\$ \(Fine Particle Dose or Respirable Mass, RM\) was calculated by interpolation. ~~Different~~ Several](#)
239 [different](#) aerodynamic parameters were [also](#) calculated: Emitted Mass, EM, the mannitol mass
240 collected from the induction port to the filter; Emitted Fraction, EF, the ratio % between the EM and
241 amount of powder loaded in the capsule; ~~Respirable Mass, RM, the mass of the aerosolized mannitol~~
242 [with an aerodynamic diameter < 5 \$\mu\text{m}\$](#) ; Respirable Fraction, RF, percentage of the RM with respect
243 to the EM. Moreover, the Mass Median Aerodynamic Diameter (MMAD) defined as the diameter

Formatted: Tab stops: 1.87", Left

244 which separates the powder in two populations with equal weight was determined by plotting the
245 cumulative percentage of mass less than the cut-off diameter for each stage on a probability scale
246 versus the relevant aerodynamic diameter of the stage on a logarithmic scale. MMAD is the slope
247 of the line obtained by linear regression of the experimental points. Finally, the Geometrical
248 Standard Deviation (GSD), a parameter indicating how wide the particle size distribution, was
249 calculated as the square root of the ratio between the size of the 84.13% of the particle population
250 in the log-normal distribution and the size of the 15.87% of the particle population in the log-normal
251 distribution.

252
253 **2.2.7 Mannitol HPLC analysis.** A Shimadzu VP (Shimadzu Corporation) high performance liquid
254 chromatographic (HPLC) system coupled with refractive index detector (RID-10A, Shimadzu) set at
255 40 °C was used for mannitol quantification, following the analytical method reported in the relevant
256 monography by United States Pharmacopeia (USP 41). Ultrapure water was employed as mobile
257 phase at a flow rate of 1 mL/min and injection volume was set at 100 µL on a Waters 717 plus
258 autosampler (Waters Corporation). As a stationary phase an Aminex[®] HPX-87H Ion Exclusion, 300
259 mm x 7.8 mm (Bio-Rad, Hercules) column was used. The column was equilibrated at 80°C for 2 hours
260 with the mobile phase pumped at 0.2 mL/min then, maintained at that temperature during the
261 chromatographic runs. A Shimadzu Class VP software was used for data acquisition and analysis.
262 Each sample was injected 6 times and the 3 closer values were used to calculate mean and standard
263 deviation. Linearity of the responses was assessed between 0.01 mg/mL and 1 mg/mL ($R^2= 0.999$).
264 The limit of detection and the limit of quantification were 2.6 µg/mL and 8 µg/mL, respectively.

265
266 **2.2.8 Fluorescent labelling of PfTrx-HPV-L2.** The PfTrx-HPV-L2 protein was dissolved in 0.1 M
267 sodium bicarbonate buffer, mixed with the reactive dye solution (Alexa Fluor 750; Life Technologies)
268 and incubated for 1 hr at RT with continuous stirring according to the manufacturer's instructions.
269 Separation of the labelled protein from the unreacted, free dye was performed by size fractionation
270 (Econo-Pac 10DG Desalting columns, Bio-Rad). Labelling stoichiometry was determined by
271 comparing the absorbance at 280 nm of equally concentrated solutions of the ~~unlabelled~~unlabeled
272 and the Alexa-labelled protein. The Alexa-conjugated PfTrx-HPV-L2 antigen incorporated into the
273 DPI at 2 % w/w of the resulting product, was administered intratracheally to female BALB/c mice, in
274 either a PBS pre-dissolved liquid form or in powder form.

275
276 **2.2.9 Animal experimentation.** Female inbred (7–8 weeks-old) BALB/c mice were purchased from
277 Envigo Laboratories (Italy). Prior to use, animals were acclimatized for at least 5 days to the local
278 vivarium conditions (room temperature: 20–24°C; relative humidity: 40–70%; 12-h light–dark cycle),
279 with free access to standard rodent chow and softened tap water. All animal experiments were
280 approved by the intramural animal welfare committee for animal experimentation (authorization n.
281 31/2015-PR to Chiesi Farmaceutici for imaging experiments; authorization n. 985/2019-PR to
282 University of Parma for immunization experiments) to comply with the European Directive 2010/63
283 UE, Italian D. Lgs 26/2014 and the revised “Guide for the Care and Use of Laboratory Animals” (Natl.
284 Res. Council, US Committee, 8th Ed, 2011).

285 For intratracheal administration, animals were lightly anesthetized with either 2.5% isoflurane
286 delivered in a transparent plastic box or ketamine/xylazine (80 and 10 mg/kg, respectively,
287 administered intraperitoneally) and positioned on the intubation platform, hanging by their incisors
288 placed on the wire. Using a small laryngoscope to visualize the trachea, the Alexa-conjugated *PfTrx*-
289 HPV-L2 vaccine was intratracheally administered by either a syringe-operated micro-cannula (liquid-
290 form vaccine) or with the use of a modified Penn-Century, Dry Powder Insufflator™ (Model DP-4M)
291 device (dry-powder vaccine) [37].
292

293 **2.2.10 *In vivo* and *ex-vivo* imaging.** Three different experimental approaches were utilized for *in*
294 *vivo* imaging. For fluorescence molecular tomography (FMT 2500; PerkinElmer), the anesthetized
295 animals were carefully positioned in the imaging cassette, which was then placed into the FMT
296 imaging chamber. A near infrared (NIR) laser diode transilluminated the thorax region (*i.e.*, passed
297 light through the body of the animal to be collected on the opposite side), and the resulting signal
298 was detected with a thermoelectrically cooled charge-coupled device camera placed on the
299 opposite side of the imaged animal. Appropriate optical filters allowed the collection of both
300 fluorescence and excitation data sets, and the multiple source-detector fluorescence projections
301 were normalized to the paired collection of laser excitation data. Cumulative fluorescence data were
302 reconstructed using the FMT 2500 system with TrueQuant software version 2.2 (Perkin Elmer) in
303 order to obtain a three-dimensional fluorescence signal quantification within the lungs.

304 The same animals were analyzed by Micro-Computed Tomography (Micro-CT) imaging, performed
305 15 min after administration with the use of a Quantum GX Micro CT apparatus (Perkin Elmer), as
306 well as by IVIS Lumina II imaging (Perkin Elmer). Micro-CT images were acquired with an intrinsic
307 retrospective two-phase respiratory gating technique using the following parameters: 90 KV, 88 μ A
308 over a total angle of 360° for a total scan time of 4 min.

309 After *in vivo* imaging, mice were euthanized by anesthetic overdosing, followed by bleeding from
310 the abdominal aorta and organ explantation. *Ex-vivo* imaging was then performed on the lungs,
311 trachea liver, ~~spleen~~spleen, and kidneys by IVIS Lumina II.

312 Portions of the explanted lungs, trachea and liver (5 mg of frozen tissue each) were suspended in
313 300 μ L of RIPA buffer [50 mM Tris-HCl, 150 mM NaCl, 1.0% (v/v) NP-40, 0.5% (w/v) Sodium
314 Deoxycholate, 0.1% (w/v) SDS, pH 8.0], disrupted by sonication (Misonix Sonicator 3000; 20 min,
315 20% power) and, after centrifugation for 20 min at 10000 x g, the resulting supernatants were
316 fractionated by SDS-PAGE, followed by detection of the Alexa-labelled *PfTrx*-HPV-L2 protein by near-
317 infrared fluorescence at 800 nm, using a ChemiDoc MP Imaging System (Bio-Rad).
318

319 **2.2.11 Animal immunization.** Mice were subdivided into four (three control and one test) groups,
320 which were injected subcutaneously (s.c.) with four doses (1 priming and 2 boosts) of a solubilized
321 control powder (#1), liquid antigen (#2), solubilized vaccine powder (#3) or the same powder
322 administered intratracheally (#4) at weekly intervals. Group #1 was comprised of five animals, which
323 were s.c. injected with 1 mg of GLA-containing but antigen-lacking powder dissolved in 50 μ L of PBS
324 right before administration. Group #2, comprised of 7 animals, was s.c. injected with the detoxified
325 and filter-sterilized liquid *PfTrx*-HPV-L2 antigen (20 μ g) adjuvanted with 50 μ g of aluminum
326 hydroxide (Brenntag) and 10 μ g of GLA. Group #3, also comprised of seven animals, was s.c. injected

327 with 1 mg of GLA-containing, *Pf*Trx-HPV-L2 vaccine powder, solubilized into 50 µL of PBS right before
328 administration Test group #4 was comprised of ten mice, to which the GLA-containing, *Pf*Trx-HPV-
329 L2-vaccine powder (about 2 mg) was administered intratracheally with the use of a modified Dry
330 Powder Insufflator™ device as described above. The average amount of vaccine powder emitted
331 from the insufflator was pre-determined by weighting the device before and after insufflation. As
332 revealed by these measurements, approximately 50% of the loaded powder was emitted from the
333 device and available for delivery; [in detail, the average amount of vaccine powder emitted from the](#)
334 [insufflator was 2.43±0.07 mg, corresponding to 48.7±1.37 µg of antigen](#). One week after the last
335 immunization (total duration of the immunization protocol: 21 days) blood samples were collected
336 by cardiac puncture, and the resulting sera, obtained by blood centrifugation (20 min at 10000 x g)
337 after 3 hr at room temperature, were used to evaluate the immune responses in ELISA and
338 neutralization assay.

339
340 **2.2.12 ELISA.** GST-Trx capture ELISA for anti-L2 antibody detection was carried out in 96-well
341 microtiter plates pre-coated with glutathione-casein and subsequently blocked with casein buffer
342 as described previously [38]. Individual immune sera were analyzed in duplicate by progressive
343 (two-fold) serial dilutions starting from a 1:50 dilution, using a pool of pre-immune sera as a control.
344 Following serum addition and 1 hr incubation at 37°C, plates were washed three times and
345 incubated with a HRP-conjugated goat anti-mouse secondary antibody (Sigma-Aldrich) previously
346 diluted 1:5000 in PBS containing 0.3% v/v Tween-20 (PBS-T). Plates were incubated for 1 h at 37°C,
347 washed three times, and developed by adding the KPL ABTS Peroxidase Substrate [2,29-azino-bis(3-
348 ethylbenz-thiazoline-6-sulfonic acid)] staining solution (SeraCare; 100 µL/well). Absorbance at 405
349 nm was measured after 30 minutes at 30°C with a microplate reader (iMark™, Bio-Rad).

350 To evaluate protein antigen integrity, 96-well microtiter plates were coated with *Pf*Trx-HPV-L2 (5
351 µg/mL in PBS, 100 µL/well; o/n incubation at 4°C) pre-exposed to different concentrations of
352 ethanol (0, 1, 5, 10, 15, 20, 30, 50, 70%) and/or to spray-drying . After three washes with PBS-T,
353 plates were blocked with 3% skim milk in PBS for 1 hr at 37°C. Serial dilutions of a monoclonal anti-
354 L2 antibody [(K4L2(20-38), [39]) [or an anti-*Pf*Trx mAb](#)] were then added, followed by three washes
355 as above and incubation for 1 hr at 37°C with a HRP-conjugated goat anti-mouse secondary antibody
356 (Sigma-Aldrich) diluted 1:5000 in PBS-T. After three additional washes, plates were developed by
357 adding the KPL ABTS Peroxidase Substrate staining solution (100 µl/well) and read at 405 nm with a
358 microplate reader after a 30 minutes incubation at 30°C (iMark™, Bio-Rad).

359
360 **2.2.13 Immunoglobulin isotyping.** Immunoglobulin subclasses in sera from mice immunized with
361 the different antigen formulations and modes of delivery were determined by ELISA using a Pierce
362 mouse antibody isotyping kit (Thermo Fisher Scientific) according to the manufacturer's
363 instructions. A pool composed by equal volumes (100 µl each) of sera from the four best responding
364 animals was employed as a test sample (50 µl fixed volume) that was added to ELISA strip-wells pre-
365 coated with isotype-specific (IgG1, IgG2a, IgG2b, IgG3, IgM, IgA) anti-mouse heavy-chain capture
366 antibodies and assayed in duplicate. Following incubation (1 hr at RT under gentle shaking
367 conditions) with horseradish peroxidase (HRP)-conjugated, goat anti-mouse IgG+IgA+IgM detection

Formatted: Font: Italic

368 antibodies and washing, the TMB substrate was added, incubated for 5-15 minutes, and color
369 development was read with a microplate reader (iMark™ Microplate Absorbance Reader, Bio-Rad)
370 at 405 nm.

371
372 **2.2.14 Neutralization assay.** L2 pseudovirion-based neutralization assays (L2-PBNA) were
373 performed as described previously [40,41]. Briefly, following MCF10A cells plating,
374 propagation/lysis, extracellular matrix (ECM) deposition and washing, a pseudovirion solution,
375 prepared in conditioned medium from CHO furin cells and supplemented with 5 µg/ml heparin
376 (Sigma H-4784) in a total volume of 120 µL/well, was added to the ECM-coated wells. The virus-
377 furin-heparin mixture was incubated overnight at 37°C. The medium was then ~~removed~~
378 and the wells were washed twice with PBS. The final wash was then replaced with the immune sera
379 (100 µL/well of the same sera utilized for immunoglobulin isotype profiling) serially diluted in pgsa-
380 745 growth medium. The plate was incubated at 37°C for 6 h to allow for antibody binding to the
381 target L2 epitope, followed by addition of pgsa-745 reporter cells (50 µL) at a concentration of
382 8×10^3 /well. For all assays, sera were serially diluted in 3-fold dilution steps starting from an initial
383 1:50 dilution. The secreted Gaussia luciferase was determined with the coelenterazine substrate
384 and Gaussia glow juice using a microplate luminometer (Victor3, PerkinElmer). Data were analyzed
385 and 50% inhibitory concentrations (IC50) were determined using the GraphPad Prism software
386 program.

387
388 **2.2.15 Statistical analysis.** Unless otherwise indicated, all values are expressed as the mean ±
389 standard deviation. Statistical significance of differences was evaluated using two-tailed unpaired t-
390 test with significance level set at a p-value ≤ 0.05. Statistical analysis was performed with Microsoft
391 Excel version 16.18 (Microsoft Corporation) and the Prism 7 software version 7.0d (GraphPad
392 Software).

Formatted: Font: Not Bold

393 3. Results and Discussion

394 3.1 Pre-formulation of respirable particles loaded with the *Pf*Trx-HPV-L2 antigen

395 Building upon previous work by Parlati et al. [23], we initially focused on the basic set-up of a DPI
396 vaccine prototype using sodium stearate as a surfactant and a technological surrogate of the
397 amphiphilic immune-adjuvant monophosphoryl lipid A (MPLA).

398 Spray-drying, which entails a temporary (in the order of milliseconds) exposure to fairly high
399 temperatures (typically from 100°C to 140 °C) and a rapid interface conversion, may be a rather
400 harsh process, especially when applied to protein-based bioactive components that may undergo
401 irreversible denaturation as well as oxidation. Based on the above considerations, in addition to the
402 use of a thermostable protein antigen, we adopted a particle engineering approach, paying special
403 attention to two key steps, namely, i) the use of a water-ethanol solution in order to dissolve the
404 amphiphilic component of the final formulation, which, on one hand, would allow to reduce the
405 inlet drying temperature but, on the other, may be detrimental to protein stability; and ii) the total
406 amount of solute in the feed solution in order to obtain a suitable amount of powder at the end of
407 the process. In fact, should the solute only be comprised of the antigen, extremely high protein
408 concentrations would be required, with protein aggregation and subsequent precipitation. We thus
409 resorted to the supplementation of the feed solution with a bulking agent. To this end, we
410 conducted a pre-formulation study with mannitol, lactose and trehalose as potential excipients. As
411 a result of this study, mannitol was selected as the best bulking agent [in the tested experimental](#)
412 [conditions](#) due the superior production yields it afforded and the superior aerodynamic
413 performance of the protein-containing powder (see Supplementary Table [S4S2](#)).

414 A further preliminary study indicated 70% v/v ethanol as the highest organic solvent content of the
415 protein-containing (*Pf*Trx-HPV-L2: 1 mg/mL) hydro-alcoholic solution compatible with protein
416 stability (see Supplementary Figure [S4S2](#)). Thus, a 70:30 (v/v), water:ethanol solution was selected
417 for the subsequent production of *Pf*Trx-HPV-L2 DPIs.

418
419 **Table 1. Manufacturing parameters and aerodynamic properties of antigen-lacking powders containing**
420 **different amounts of sodium stearate¹**

Powder #	Sodium Stearate (% w/w)	pH of Feed Solution	Yield (%)	D _{v,50}	EF (%)	RF (%)
1	-	5.89	54.63	6.08 (0.74)	87.51 (2.01)	43.52 (4.01)
2	0.33	5.88	31.53	18.58 (2.44)	75.16 (5.17)	8.02 (3.04)
3	1.00	7.94	43.72	3.40 (0.73)	89.89 (1.32)	48.10 (9.39)
4	2.00	8.14	59.46	26.35 (3.09)	94.46 (2.69)	13.59 (7.21)

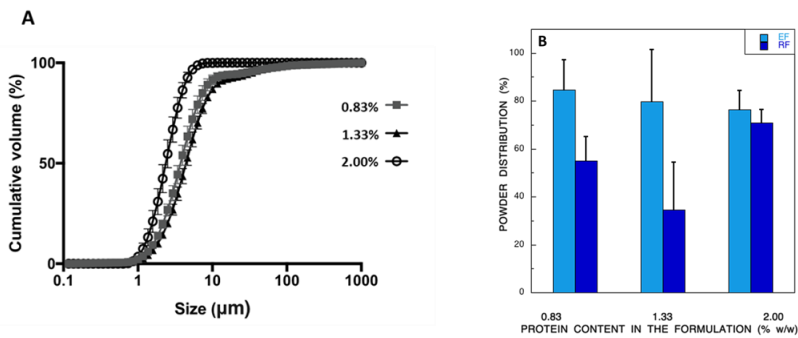
421
422 ¹Sodium stearate content (as percentage by weight of the solutes contained in the feed solution), production yield, pH of the feed solutions, median
423 volume diameter (D_{v,50}), Emitted Fraction (EF, as percentage of the loaded amount) and Respirable Fraction (RF, as percentage of the loaded amount)
424 of powders prepared with different amounts of sodium stearate. Mean values and standard deviations in parenthesis (n=3).

425

426 In parallel, the concentration of sodium stearate in the feed solution (from 0.33 to 2.00% w/w of
427 the solute) was investigated with respect to the particle size distribution (Table 1) and *in vitro* (fast
428 screening) deposition of the resulting powders. The respirability vs sodium stearate concentration
429 profile could be fitted to a quadratic equation with a maximum around 1% w/w sodium stearate,
430 thus confirming previous data obtained in a similar experimental set-up [23].

431 Based on these pre-optimized experimental conditions, we then investigated the effect of an
432 increased antigen content (i.e., a *Pf*Trx-HPV-L2 starting concentration higher than 1 mg/ml and a
433 correspondingly higher fractional protein content) on the physico-chemical properties of the
434 resulting powders [prepared with 1% sodium stearate](#). Three antigen concentrations, expressed as
435 solute weights in the feed solution of 0.83, 1.33 and 2.00% w/w, were tested ([Powders #3a, #3b and](#)
436 [#3c](#)). The particle size distribution and the aerodynamic behavior of the resulting powders are
437 reported in Figure 1.

438



439

440 **Figure 1. (A)** Particle cumulative undersize distribution evaluated by laser light diffraction of spray-dried
441 powders [3a, #3b and #3c](#) containing different amounts of the antigen: 0.83% w/w (*squares*), 1.33% w/w
442 (*triangles*), 2.00% w/w (*empty circles*) (mean values and standard deviation bars are indicated; n=3). **(B)**
443 Emitted fraction (EF) and Respirable Fraction (RF) aerodynamic properties of three powders containing
444 different amounts of the *Pf*Trx-HPV-L2 antigen as indicated. Mean and standard deviation values (n=3) are
445 indicated.

446

447 At a 2.00% w/w antigen concentration (obtained by adding 1.5 mL of an 8 mg/mL protein solution
448 to 100 mL of feed solution), a monomodal powder (span 1.28 ± 0.04 , Figure 1A) composed of highly
449 respirable microparticles (RF=70.9% \pm 5.6) (Figure 1B) was produced, with a spray-drying yield of
450 approximately 65%. SDS-PAGE analysis (Figure 2A) confirmed the presence of an apparently intact,
451 dry-powder associated antigen, whose functional integrity (i.e., the ability to be recognized by anti-
452 HPV-L2 and anti-*Pf*Trx mAbs) was verified by ELISA (Figure 2B).

453

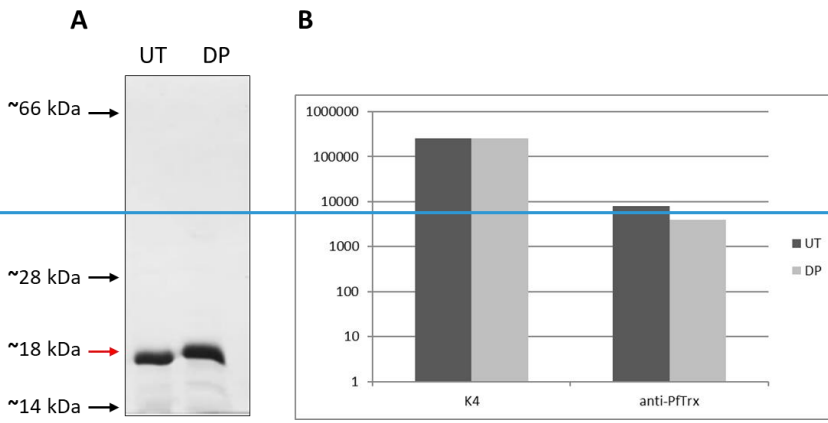
Formatted: Font: Italic

Formatted: Font: Italic

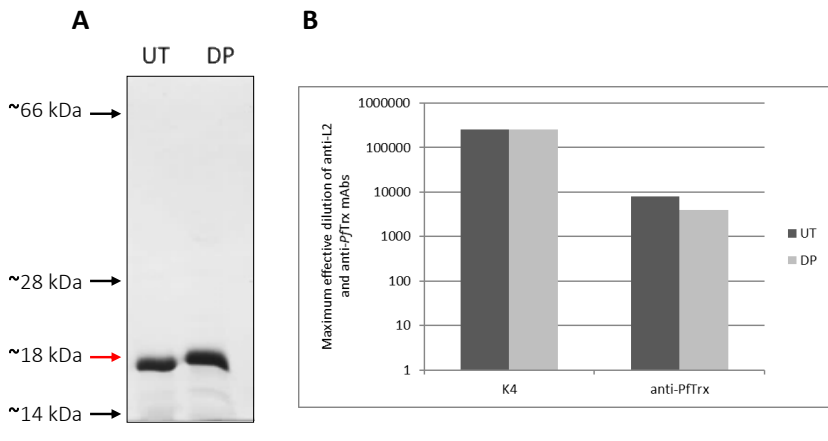
Formatted: Font: Italic

Formatted: Font: Italic

454



455



456

Figure 2. (A) SDS-PAGE analysis of the untreated (UT) liquid-form and the dry-powder formulated (DP) *PfTrx*-HPV-L2 antigen. The expected migration position of the *PfTrx*-HPV-L2 protein is indicated by a red arrow, the slight difference in electrophoretic mobility between the UT and the DP samples is due to a migration artifact; the migration positions of molecular mass markers are indicated by black arrows. **(B)** Comparative ELISA analysis of the immunoreactivity of the untreated (UT, dark-grey) and the dry-powder formulated (DP, light-grey) *PfTrx*-HPV-L2 antigen. mAbs directed against the L2 epitope (K4) or the *Pyrococcus* thioredoxin scaffold (anti-*PfTrx*) were used as primary antibodies. The results are the average of two technical replicates, which differed by no more than 5% from of the mean.

464

465

466

467

468

3.2 Conversion of *PfTrx*-HPV-L2 into a prototype respiratory vaccine using GLA as a particle lubricant and a built-in immune-adjuvant

469

470

The presence of an immune-adjuvant is an essential prerequisite for subunit vaccine immunogenicity [1,2], including vaccines such as Gardasil and Cervarix that are made up by

Formatted: Font: Italic

Formatted: Font: Italic

Formatted: Font: Italic

Formatted: Font: Italic

Formatted: Font: Italic

Formatted: Font: Italic

Formatted: Font: Italic

Formatted: Font: Italic

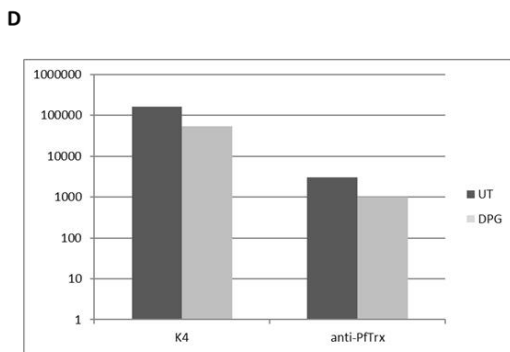
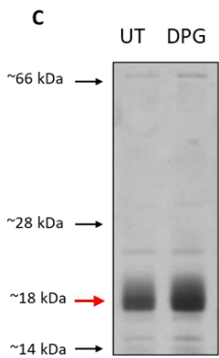
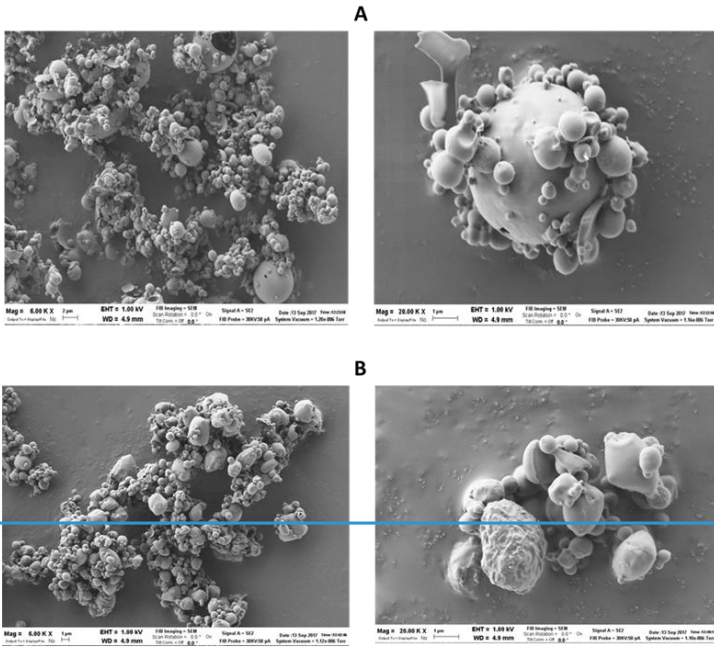
Formatted: Font: Italic

Formatted: Font: Italic

471 intrinsically highly immunogenic HPV-L1 pseudovirion components [25,26,28]. GLA is a synthetic
472 derivative of MPLA, a low-toxicity lipopolysaccharide that is present as a biological adjuvant in
473 various licensed vaccines, including Cervarix. GLA is an amphiphilic molecule that acts as an agonist
474 of toll-like receptor 4 (TLR4) [42]. GLA itself [43] and its parent compound MPLA [20,27,44] have
475 proved to be effective immune adjuvants when included in formulations for nasal and pulmonary
476 administration. The amphiphilic nature of GLA prompted us to test its possible use as a sodium
477 stearate replacement, capable of acting as both a coating agent enhancing particle flow, de-
478 aggregation and ultimately respirability, as well as a built-in immune-adjuvant.

479 We thus set out to incorporate GLA as a sodium stearate substitute in our PfTrx-HPV-L2
480 microparticle formulation. As a first approximation, we estimated the amount of GLA that would be
481 required to obtain a particle surface coating ~~similar to~~like that achieved with sodium stearate,
482 ~~starting from the assumption that a lower amount of a larger molecule is needed to cover the same~~
483 ~~surface~~. Based on the molecular weight ratio between ~~sodium stearate (306.5 g/mol) and~~ GLA
484 (1763.5 g/mol) ~~and sodium stearate (306.5 g/mol)~~, a 1% (w/w) fractional amount of sodium stearate
485 corresponds to approximately 0.17% w/w GLA. With respect to the GLA concentration in the feed
486 solution, this amount corresponds to 1.02 µg/ml, which is one order of magnitude lower than the
487 reported CMC for MPLA [45]. Thus, also considering that the feed solution contained 30% v/v
488 ethanol, we assumed that GLA was completely dissolved without micelle formation, which
489 represents a key feature for the surfactant migration at the air/liquid interface of the droplets during
490 the spray-drying process [23,46,47]. The adjuvant concentration we employed is significantly higher
491 than that reported in the literature [20], thus allowing to assume that a relevant portion of GLA
492 distributed to the droplet air liquid interface during the drying process and, ultimately, on the
493 microparticle surface.

494 A new powder, containing GLA as both an amphiphilic technological excipient with particle lubricant
495 functionality and an immune adjuvant, was thus produced, starting from 4 and 12 mg/mL solutions
496 of detoxified and filter-sterilized PfTrx-HPV-L2 antigen dissolved in phosphate buffer. In this way, an
497 antigen concentration in the final powder of 1.33% w/w (Powder #5) or 2 % w/w (Powder #6) was
498 obtained.



513 concentration (Figures 3A and 3B), featured a narrow mono-modal size distribution: ~~with a for~~
514 ~~Powder #5~~ $D_{v,10} = 1.27 \pm 0.12 \mu\text{m}$, $D_{v,50}$ of $2.39 \pm 0.24 \mu\text{m}$, $D_{v,90} = 4.30 \pm 0.32 \mu\text{m}$, Span value = 1.27; for
515 Powder #5-6 and $D_{v,10} = 1.43 \pm 0.09 \mu\text{m}$, $D_{v,50} = 2.65 \pm 0.18 \mu\text{m}$, $D_{v,90} = 4.78 \pm 0.55 \mu\text{m}$, Span value =
516 1.26 for Powder #6. The solution obtained upon particle solubilization in ultrapure water displayed
517 a slightly basic pH (7.5 and 8.0 for Powder #5 and #6, respectively).

518 ~~The lubricant functionality of GLA was compared to that of sodium stearate by evaluating the~~
519 ~~powder flow properties through the determination of the dynamic angle of repose according to Ph.~~
520 ~~Eur. 10th ed. The measurement was carried out on powders containing the same amount of antigen~~
521 ~~(1.33%). The GLA-containing powder had an angle of repose of $18.74 \pm 1.48^\circ$ indicative of excellent~~
522 ~~flow properties, as opposite to the sodium stearate-containing powder which showed poor~~
523 ~~flowability (angle of repose = $46.6 \pm 0.60^\circ$).~~

524 Aerosolization performance analysis, initially conducted with the RS01[®] device and a Fast Screening
525 Impactor (FSI), yielded an Emitted Fraction (EF) of $86.0\% \pm 0.8$ (Powder #5) and $81.3\% \pm 11.2$
526 (Powder #6) and a Fine Particle Fraction (FPF) of $61.2\% \pm 8.6$ (Powder #5) and $60.0\% \pm 2.0$ (Powder
527 #6).

528 To gain more detailed information on the aerodynamic particle size distribution of powder #6 (~~the~~
529 ~~one with the highest antigen content~~), aerodynamic performance was also assessed with an
530 Andersen Cascade Impactor (ACI) through quantitative detection of mannitol in the impactor stages
531 by a HPLC/RID method. Since the protein is embedded within GLA-coated, mannitol-containing
532 particles, it was assumed that mannitol could be used as a reliable indicator of antigen emission
533 from the device and its distribution within the different stages of the impactor. Mannitol emitted
534 from RS01[®] was 12.5 ± 1.5 mg (EF = $64.2\% \pm 7.85$), with a Fine Particle Mass (FPM) of approximately
535 9 ± 0.7 mg (RF = $72.3\% \pm 5.59$) and a Median Mass Aerodynamic Diameter (MMAD) of $2.5 \pm 0.1 \mu\text{m}$.

536 A subset of powder #6-filled capsules was stored at room temperature under light-shielded
537 conditions and re-tested 5 months after production. The mannitol EF was found to be approximately
538 10% higher compared to time zero; RF also increased ($83.2\% \pm 12.1$), ~~although for both parameters~~
539 ~~the difference was not statistically significant with respect to the values recorded at time zero~~
540 ~~($p > 0.5$); ~~whereas the~~ MMAD remained essentially the same. ~~Surprisingly, a better aerodynamic~~
541 ~~performance was observed after storage, likely due to either loss of residual humidity or surface~~
542 ~~charge dissipation and a consequent improvement of powder deaggregation upon aerosolization.~~~~

543 The presence of residual free water was excluded by Thermo-Gravimetric Analysis, which indicated
544 a negligible water loss ($< 0.1\%$) upon heating (not shown), while Isothermal Dynamic Vapor Sorption
545 measurements carried out at both 25°C and 40°C revealed the very low and completely reversible
546 tendency of the powder to absorb humidity (see Supplementary Figure S2). This can be ascribed
547 both to the partial hydrophobic coating of the particle surface with GLA and to the fact that the
548 spray-drying process yielded the β -form of mannitol (melting peak at 166°C revealed by DSC
549 analysis; not shown), which represents the thermodynamically stable and non-hygroscopic crystal
550 form of the bulking agent (i.e., the most abundant component of the powder). As revealed by semi-
551 quantitative SDS-PAGE analysis (Figure 3C), the PflTrx-HPV-L2 content of the GLA powder was in line
552 with the amount expected ~~on the basis of~~ based on the input concentration and fractional content
553 of the protein. Importantly, the immunoreactivity of the solubilized spray-dried antigen (i.e., the

Formatted: Superscript

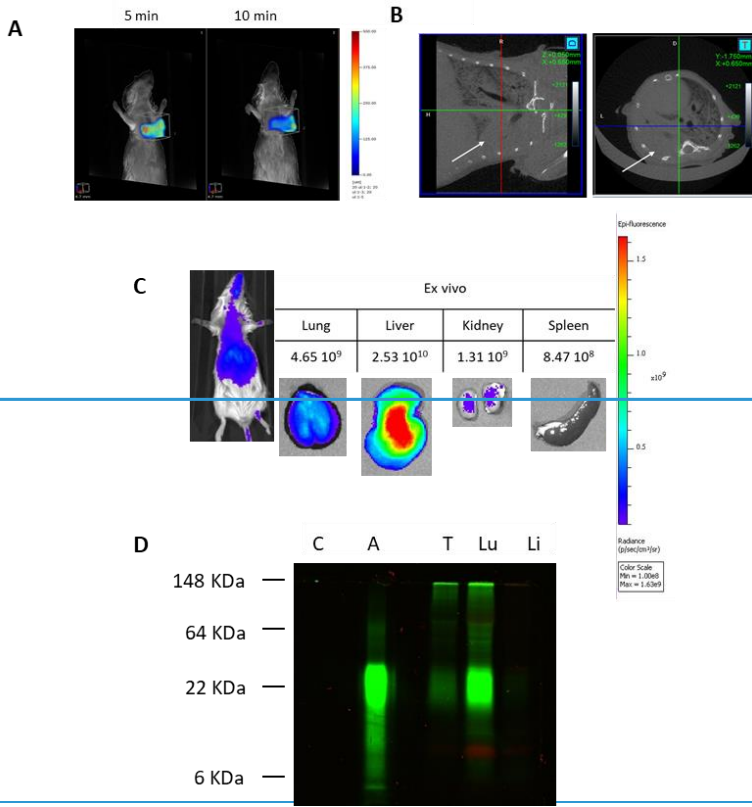
554 antigen retrieved from particles dissolved in aqueous buffer) revealed by ELISA was the same as that
555 of the native antigen (Figure 3D).

556

557 **3.3 Lung deposition of the *Pf*Trx-HPV-L2-[GLA] dry-powder vaccine administered intratracheally**

558 To gain insight on the lung deposition capacity of the *Pf*Trx-HPV-L2-[GLA] vaccine (Powder #6)
559 administered intratracheally, we set-up conditions for direct *in vivo* imaging of the antigen. To this
560 end, we used the NIR-dye Alexa Fluor 750 to label the *Pf*Trx-HPV-L2 protein. The labeled protein
561 was then incorporated into GLA-coated particles using the previously developed formulation
562 procedure (spray-dry yield of 57.8% w/w). Prior to intratracheal delivery, the powder was subjected
563 to an FSI aerodynamic evaluation, which yielded Emitted Fraction and Respirable Fraction values
564 ($87.2\% \pm 6.1$ and $67.0\% \pm 4.8$, respectively) superimposable to those obtained with the unlabeled
565 protein-containing powder.

566



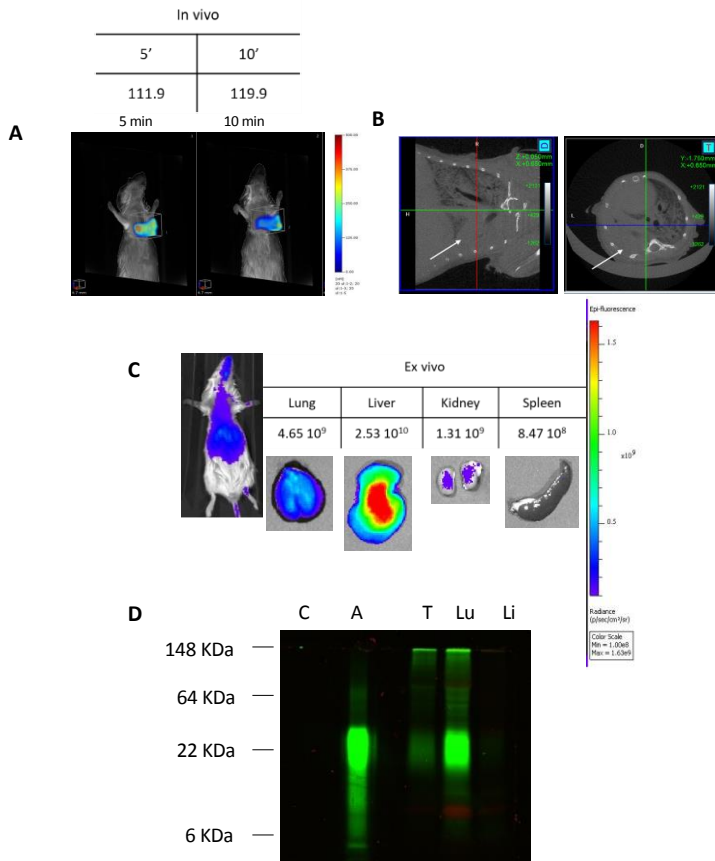


Figure 4. Tissue distribution of the Alexa Fluor750-labeled *PfTrx*-HPV-L2 antigen delivered intratracheally in liquid form. Intratracheally administered, pre-dissolved Alexa-labeled vaccine powder visualized by FMT, 5 and 10 min after intratracheal delivery (**A**) and by Micro-CT (**B**) imaging (transversal and coronal views are shown in the left- and right-side images, respectively, where the arrows indicate the accumulation sites of the delivered liquid vaccine). *In vivo* (**C**, left-side panel) and *ex-vivo* multi-organ (**C**, right-side panel) IVIS imaging of the Alexa-labeled *PfTrx*-HPV-L2 antigen 15 min after intratracheal administration. (**D**) SDS-PAGE fractionation and fluorescence-based visualization of trachea (T), lung (Lu) and liver (Li) tissue homogenates derived from a mouse, to which the pre-dissolved, Alexa-labeled dry-powder vaccine was administered intratracheally; equivalent amounts (5 ng) of the unlabeled (C) and the Alexa-labeled (A); *PfTrx*-HPV-L2 protein served as controls for this experiment. The results are from a representative experiment that was performed in parallel on two different animals.

In a preliminary experiment aimed at setting-up mouse pulmonary administration conditions, the labeled dry-powder vaccine was dissolved in aqueous buffer prior to intratracheal delivery. As shown in Figure 4A, the Alexa-labeled *PfTrx*-HPV-L2 protein could be tracked in the lungs by FMT,

Formatted: Font: Italic

Formatted: Font: Not Bold

Formatted: Font: Not Bold, Italic

Formatted: Font: Not Bold

Formatted: Font: Not Bold, Italic

Formatted: Font: Italic

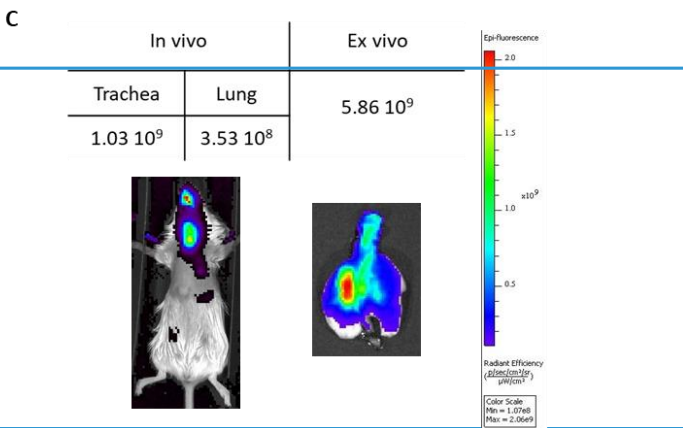
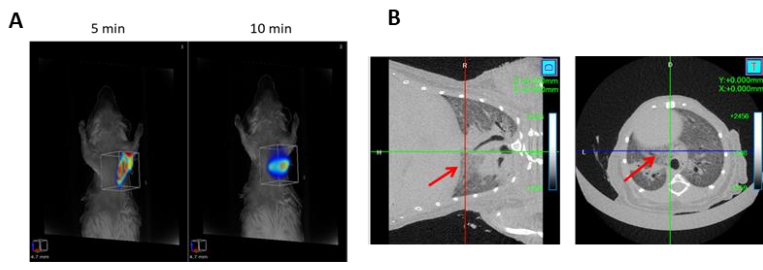
Formatted: Font: Italic

585 with nearly the same fluorescence intensity at 5 and 10 min after delivery and a slightly preferential
586 (but likely random) accumulation in the left lobe. This kind of distribution was confirmed by Micro-
587 CT imaging, which alloweds to visualize the fine anatomical details of the lung delivery site (Figure
588 4B). As revealed by IVIS imaging, after 15 min the fluorescence signal became more diffuse and
589 apparently spread to the liver and other sub-thoracic organs (Figure 4C). Indeed, an intense
590 fluorescence was detected not only in the lungs but also in the liver and other organs explanted
591 after mouse sacrifice. To distinguish between protein-associated fluorescence and a spurious signal
592 arising from protein degradation and release into the circulation of the Alexa dye (either free or
593 associated to *PfTrx*-HPV-L2 peptide fragments), trachea, lung and liver tissue homogenates from the
594 same animal were examined by SDS-PAGE. As shown in Figure 4D, a strong and a slightly weaker
595 but well detectable fluorescence signal was found to be associated -in lung and trachea extracts,
596 respectively- with a polypeptide displaying the same electrophoretic mobility as the authentic
597 Alexa-labeled *PfTrx*-HPV-L2 protein, whereas no fluorescence was detected in the case of the liver
598 homogenate. This indicates that liver fluorescence was indeed associated to small-sized degradation
599 products of the labeled *PfTrx*-HPV-L2 protein, that ran out of the gel upon electrophoretic
600 fractionation.

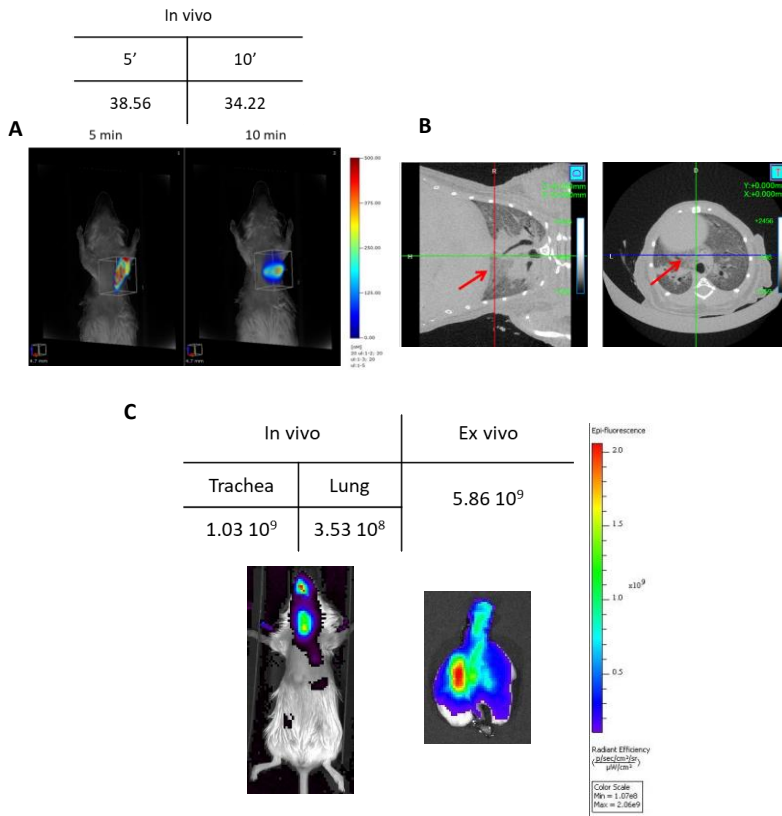
601 Next, a similar experiment was conducted with the *PfTrx*-HPV-L2-[GLA] powder (2 mg containing 12
602 µg of Alexa-labelled antigen), delivered intratracheally with the use of a modified dry powder
603 insufflator device. As shown by the data presented in Figure 5, also under these conditions, which
604 closely mimic the actual set-up of mouse pulmonary vaccination, a fairly even antigen distribution
605 within the respiratory tract, with a marked accumulation in the lungs, was revealed by *in-vivo* and
606 *ex-vivo* analyses. Specifically, *in vivo* imaging by FMT revealed fluorescence signals of similar
607 intensity in the lungs at both 5 and 10 min after administration (Figure 5A). A more targeted
608 localization to the chest region compared to the solubilized vaccine was revealed by IVIS imaging
609 (*cf.* Figure 5C with Figure 4C). As shown in Figure 5B, these results were confirmed by the more
610 anatomically detailed visualization afforded by Micro-CT analysis.

611 Altogether, these data fully support the favorable aerodynamic properties and suitability for
612 pulmonary administration of the *PfTrx*-HPV-L2-[GLA] powder initially pointed out by the results of
613 *in vitro* aerosolization analyses.

614



615



616

617

618 Figure 5. Lung deposition of the intratracheally administered dry-powder vaccine. (A) *In vivo* total body FMT
 619 imaging of the Alexa Fluor750-labelled *PfTrx*-HPV-L2 antigen distribution at two different time-points (5 and
 620 10 min) after administration of the vaccine powder. (B) Micro-CT imaging of antigen deposition into the lungs;
 621 transversal and coronal views are shown in the left- and right-side images, respectively, where the arrows
 622 indicate the vaccine powder deposition sites. (C) *In vivo* (left panel) and *ex-vivo* (right panel), IVIS analysis of
 623 Alexa Fluor 750-labelled *PfTrx*-HPV-L2 accumulation in the respiratory tract, 15 min after intratracheal
 624 delivery of the dry-powder vaccine.

625

626 **3.4 Preliminary evaluation of the immunogenicity of the pulmonary delivered *PfTrx*-HPV-L2-[GLA]
 627 dry-powder vaccine**

628 A comparative, pulmonary vs. subcutaneous (s.c.) vaccination experiment was then set-up. ~~In~~
 629 ~~addition to the test sample (#4), i.e., the *PfTrx*-HPV-L2-[GLA] dry powder vaccine administered~~
 630 ~~intratracheally,~~ This included the following treatment and control groups: group #1 s.c. injection of
 631 a solubilized, GLA-containing dry-powder lacking the antigen (negative control); group #2 s.c.

Formatted: Font: Italic

Formatted: Font: Italic

Formatted: Font: Italic

Formatted: Font: Italic

Formatted: Not Strikethrough

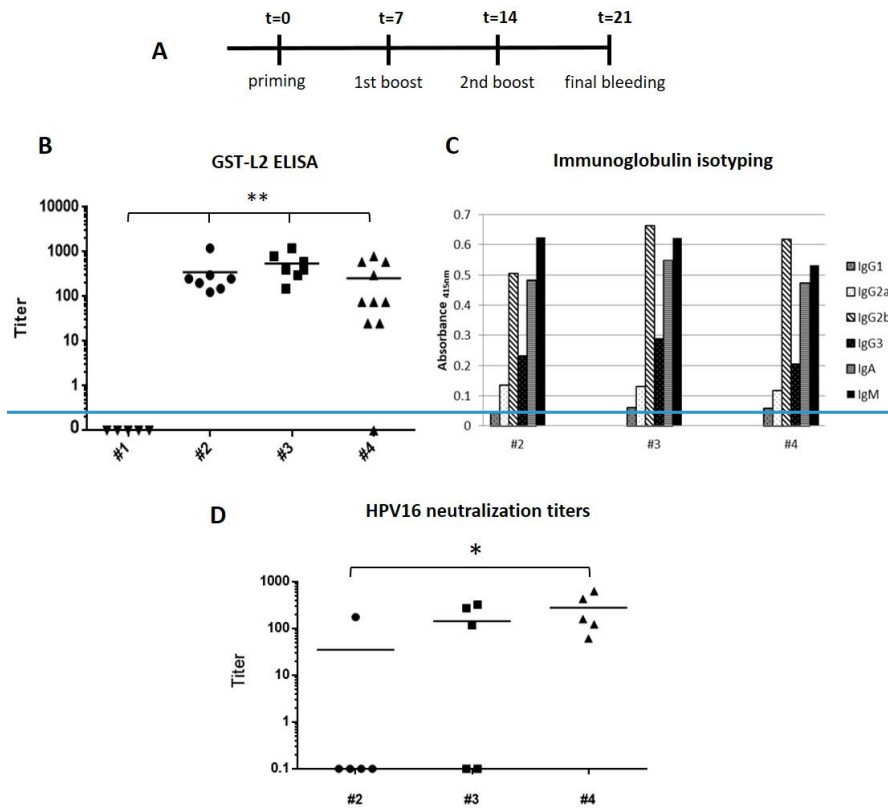
Formatted: Not Highlight

Formatted: Not Highlight

632 injection of the liquid-~~form~~, alum+GLA-adjuvanted *Pf*Trx-HPV-L2 antigen; [group #3](#)) s.c. injection of
633 the *Pf*Trx-HPV-L2-[GLA] dry-powder vaccine solubilized immediately before administration; [group](#)
634 ~~[#4 the *Pf*Trx-HPV-L2-\[GLA\] dry-powder vaccine administered intratracheally.](#)~~

Formatted: Not Strikethrough

635



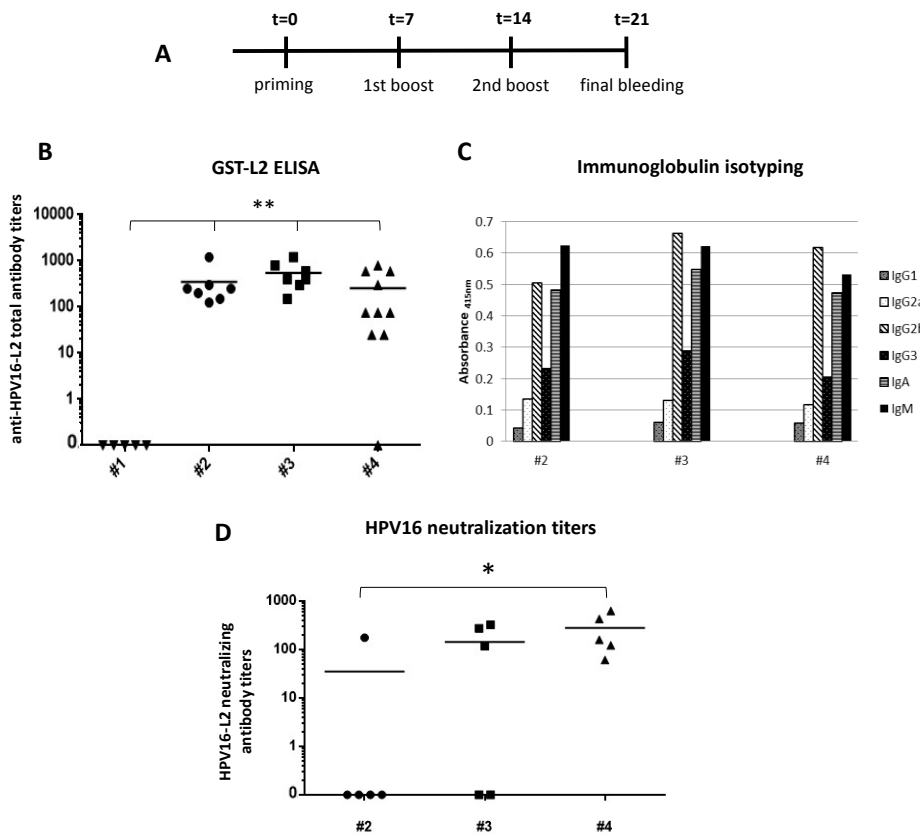


Figure 6. Immunogenicity profiling. **(A)** Timeline of the short-term immunization experiment performed with the GLA-adjuvanted, PflTrx-HPV-L2 DPI delivered intratracheally. **(B)** GST-L2 ELISA performed on sera from differently treated groups of mice, collected one week after the last immunization. The following treatments were applied to individual groups: #1, negative control, subcutaneous immunization with solubilized, GLA only containing powder with no antigen; #2, subcutaneously injected, liquid form, GLA+alum adjuvanted PflTrx-HPV-L2 antigen; #3 subcutaneously injected PflTrx-HPV-L2-[GLA] dry-powder vaccine solubilized in PBS immediately before administration; #4, PflTrx-HPV-L2-[GLA] dry-powder vaccine administered intratracheally. Data represent anti-HPV-L2 total antibody titers measured in individual mice; the means of the titers for each group are indicated by horizontal lines (** $p \leq 0.01$). **(C)** Immunoglobulin isotyping of pooled sera from the mice groups (#2, #3 and #4) shown in panel B, with the exception of except for the completely unresponsive, negative control group #1. **(D)** HPV16 neutralization titers determined by the L2-PBNA on a subset of five immune-sera/group (#2, #3 and #4) derived from the animals in each group that displayed the highest (top five) anti-HPV-L2 total antibody titers by GST-L2 ELISA (panel B). Data represent neutralizing antibody titers measured in individual mice; mean values of the titers for each group are indicated by horizontal lines (* $p \leq 0.05$).

Formatted: Font: Italic

Formatted: Font: Italic

655
656 ~~In order to~~To minimize the risk (and potential confounding effects) of bacterial infections associated
657 to intratracheal delivery, we decided to use a short-schedule immunization protocol. This only
658 involved two boost immunizations at a one-week interval, followed by final bleeding and immune
659 sera collection after one more week (Figure 6A). As shown by the ELISA data reported in Figure 6B,
660 very similar titers of total anti-L2 antibodies were detected in all groups, except for the antigen-
661 lacking, negative control. The fact that absolute titers (average value=1:370) were significantly lower
662 than those detected previously with the same antigen delivered subcutaneously [48] is likely
663 explained by the short-term immunization protocol adopted in the present exploratory study (21
664 days with only two boost injections and final bleeding all one-week a part), compared to 72 days
665 with three biweekly boost injections and a 1-month time-interval before sera collection [31,32,34].
666 We also determined the immunoglobulin isotype-profile of the antibodies elicited by the different
667 immunogens and modes of delivery. As shown in Figure 6C, the immunoglobulin isotype
668 distributions associated to the dry-powder and the liquid vaccines were quite similar. In both cases,
669 the Th1-associated IgG2b and IgG3 isotypes were considerably (10-fold on average) more
670 represented than the Th2-associated IgG1 isotype. This indicates a marked Th1 polarization of the
671 immune response that was previously shown to be causally associated to the use of the GLA
672 immune-adjuvant [42,43]. Also highly represented were the IgM and IgA immunoglobulins, with a
673 slight prevalence of the latter isotype in the case of the dry-powder vaccine.
674 Despite the short immunization schedule employed for this exploratory experiment, we also
675 determined the ability of the induced anti-L2 antibodies to neutralize HPV16 pseudovirions. To this
676 end, we used the highly sensitive L2-based pseudovirion neutralization assay [41] to determine the
677 presence of HPV16 neutralizing antibodies. As shown in Figure 6D, the highest and most consistent
678 titer (5 positives out of 5 tested serum samples) was detected in sera from mice immunized
679 intratracheally with the dry-powder formulation (#4). Interestingly, a slightly lower and less
680 consistent (3 positives out of 5 tested sera) but well detectable neutralizing response was also
681 observed in mice subcutaneously immunized with the solubilized dry-powder vaccine (#3). Instead,
682 a poor neutralizing response, with only one out of five tested sera capable of HPV16 pseudovirion
683 neutralization, was observed for sera from mice immunized subcutaneously with the liquid vaccine
684 formulation (#2). The latter result, which contrasts with the neutralization capacity previously
685 documented for the liquid-form, Montanide ISA720-, Alum/MPLA- or AddaVax-adjuvanted *PfTrx*-
686 HPV-L2 antigen administered subcutaneously using the standard 72 days immunization protocol
687 [31,32,34,48], likely reflects the short-term immunization schedule utilized for this experiment and
688 perhaps the lack of an adequate length of time for antibody affinity-maturation. Under these sub-
689 optimal but highly stringent immunization conditions, the dry-powder formulated *PfTrx*-HPV-L2-
690 [GLA] vaccine administered intratracheally, thus appears to be superior to the liquid-form vaccine,
691 at least with respect to the short-term induction of HPV16 neutralizing antibodies.
692

4. Conclusions

We have provided proof-of-concept validation of a novel particle engineering approach that allows to produce a highly respirable powder vaccine by exploiting GLA as a double-purpose component capable of acting as both a technological lubricant improving the aerodynamic properties of the powder and an immune adjuvant. Both features stem from the amphiphilic nature of the GLA molecule that partitions on the particle surface during spray-drying manufacturing.

We also exploited the thermostability of the *Pf*Trx-HPV-L2 antigen, which proved to be resistant to a fairly high ethanol concentration, for immediate drying of a mannitol-supplemented, antigen-containing solution. The resulting dry-powder vaccine, which was always handled under non-refrigerated conditions, did not change its physico-chemical or aerodynamic properties, and retained a fully intact antigen upon storage for five months at room temperature. Indirect evidence, such as powder vaccine immunogenicity and the marked Th1 polarization of the induced immune response, indicates that the relatively harsh conditions associated to spray-drying are also well tolerated by the GLA adjuvant.

An open question regards the applicability of the present approach to other, less sturdy antigens. However, preliminary results (not presented in this work) indicate that a good quality and immunogenic dry powder vaccine could also be obtained with a more complex and less thermostable antigen, in which *Pf*Trx-HPV-L2 is genetically fused to an oligomerization domain that converts the primary antigen into a heptameric nanoparticle form [49-50].

Pulmonary delivered powder vaccines have often been found to induce a superior immune response compared to their parenterally injected counterparts [7,21,22]. It is thus not so surprising that even in our preliminary, and largely sub-optimal immunization experiments, the intratracheally administered DPI vaccine outperformed the subcutaneously injected vaccine in the short-term induction of HPV16 neutralizing antibodies. The reasons for this apparent superiority remain to be clarified. They might be related to either the particulate nature of a dry-powder vaccine, which has previously been shown to enhance immunogenicity through a more efficient targeting of antigen presenting cells [7,21], the closer physical association between the antigen and the GLA adjuvant inherent to the dry powder formulation, and/or to the large surface area and extensive vascularization of the lungs [18]. Interestingly, even the DPI vaccine solubilized right before subcutaneous injection, induced higher and more consistent neutralizing antibody titers than its liquid-form counterpart. Whether this is due to residual micro-particle aggregates that resisted complete dissolution or to a tighter association between the GLA adjuvant and the antigen is presently not known. Also unknown, and worth of future, more detailed investigations is the ability of the *Pf*Trx-HPV-L2 vaccine (and its polytopic derivatives [49-50]) to induce a mucosal response in the lungs, but also in the genital apparatus. This, together with a more extensive characterization of the HPV neutralizing immune responses elicited by a longer-term immunization protocol, will also shed light on the cross-neutralization potential of the pulmonary delivered *Pf*Trx-HPV-L2 vaccine. Altogether, the data presented in this work represent a step forward toward the development of needle-free and easy to handle, next-generation vaccines.

733 **Acknowledgments**

734 GS was partly supported by a post-doc fellowship from the Interuniversity Consortium for
735 Biotechnology (CIB). This work, which also benefited from the resources made available within the
736 COMP-HUB Initiative, funded by the “Departments of Excellence” program of the Italian Ministry
737 for Education, University and Research (MIUR, 2018–2022), was supported by a Regione Emilia
738 Romagna POR-FESR grant (PG/2015/731196) to SO and RB.

739

740 **Conflicts of interest**

741 The authors declare no conflict of interest. A European patent application based on the results of
742 this study has been filed (WO2019EP78277).

743

744

745

References

746

- 747 [1] P. Piot, H.J. Larson, K.L. O'Brien, J. N'kengasong, E. Ng, S. Sow, et al., Immunization: vital
748 progress, unfinished agenda, *Nature*. 575 (2019) 119–129. doi:10.1038/s41586-019-1656-
749 7.
- 750 [2] R. Rappuoli, M. Pizza, G. Del Giudice, E. De Gregorio, Vaccines, new opportunities for a new
751 society, *Proc. Natl. Acad. Sci. U.S.a.* 111 (2014) 12288–12293. doi:10.1073/pnas.1402981111.
- 752 [3] R. Rappuoli, E. De Gregorio, G. Del Giudice, S. Phogat, S. Pecetta, M. Pizza, et al., Vaccinology
753 in the post-COVID-19 era, *Proc. Natl. Acad. Sci. U.S.a.* 118 (2021).
754 doi:10.1073/pnas.2020368118.
- 755 [4] C. Clendinen, Y. Zhang, R.N. Warburton, D.W. Light, Manufacturing costs of HPV vaccines
756 for developing countries, *Vaccine*. 34 (2016) 5984–5989.
757 doi:10.1016/j.vaccine.2016.09.042.
- 758 [5] World Health Organization, *The controlled temperature chain (CTC): frequently asked
759 questions*,
760 https://www.who.int/immunization/programmes_systems/supply_chain/resources/Controlled-Temperature-Chain-FAQ.pdf?ua=1 (accessed 2021, January 31st).
- 761 [6] Y. Nir, A. Paz, E. Sabo, I. Potasman, Fear of injections in young adults: prevalence and
762 associations, *Am J Trop Med Hyg.* 68 (2003) 341–344.
- 763 [7] T. Sou, E.N. Meeusen, M. de Veer, D.A.V. Morton, L.M. Kaminskas, M.P. McIntosh, New
764 developments in dry powder pulmonary vaccine delivery, *Trends in Biotechnology*. 29
765 (2011) 191–198. doi:10.1016/j.tibtech.2010.12.009.
- 766 [8] D.A. LeClair, E.D. Cranston, Z. Xing, M.R. Thompson, Optimization of Spray Drying Conditions
767 for Yield, Particle Size and Biological Activity of Thermally Stable Viral Vectors,
768 *Pharmaceutical Research*. 33 (2016) 2763–2776. doi:10.1007/s11095-016-2003-4.
- 769 [9] S. Ohtake, R.A. Martin, L. Yee, D. Chen, D.D. Kristensen, D. Lechuga-Ballesteros, et al., Heat-
770 stable measles vaccine produced by spray drying, *Vaccine*. 28 (2010) 1275–1284.
771 doi:10.1016/j.vaccine.2009.11.024.
- 772 [10] T. Sou, D.A.V. Morton, M. Williamson, E.N. Meeusen, L.M. Kaminskas, M.P. McIntosh, Spray-
773 Dried Influenza Antigen with Trehalose and Leucine Produces an Aerosolizable Powder
774 Vaccine Formulation that Induces Strong Systemic and Mucosal Immunity after Pulmonary
775 Administration, *J Aerosol Med Pulm Drug Deliv.* 28 (2015) 361–371.
776 doi:10.1089/jamp.2014.1176.
- 777 [11] D.A. LeClair, E.D. Cranston, Z. Xing, M.R. Thompson, Evaluation of excipients for enhanced
778 thermal stabilization of a human type 5 adenoviral vector through spray drying,
779 *International Journal of Pharmaceutics*. 506 (2016) 289–301.
780 doi:10.1016/j.ijpharm.2016.04.067.
- 781 [12] S. Afkhami, D.A. LeClair, S. Haddadi, R. Lai, S.P. Toniolo, H.C. Ertl, et al., Spray dried human
782 and chimpanzee adenoviral-vectored vaccines are thermally stable and immunogenic in
783 vivo, *Vaccine*. 35 (2017) 2916–2924. doi:10.1016/j.vaccine.2017.04.026.
- 784 [13] F. Emami, A. Vatanara, E.J. Park, D.H. Na, Drying Technologies for the Stability and
785 Bioavailability of Biopharmaceuticals, *Pharmaceutics*. 10 (2018) 131.
786 doi:10.3390/pharmaceutics10030131.
- 787
- 788

Formatted: English (United Kingdom)

Field Code Changed

- 789 [14] M.L. Levy, W. Carroll, J.L. Izquierdo Alonso, C. Keller, F. Lavorini, L. Lehtimäki, Understanding
790 Dry Powder Inhalers: Key Technical and Patient Preference Attributes, *Adv Ther.* 36 (2019)
791 2547–2557. doi:10.1007/s12325-019-01066-6.
- 792 [15] M.L. Cohn, C.L. Davis, G. Middlebrook Airborne immunization against tuberculosis, *Science.*
793 128 (1958) 1282–1283. doi:10.1126/science.128.3334.1282.
- 794 [16] R.H. Waldman, J.J. Mann, P.A. Small, Immunization against influenza. Prevention of illness
795 in man by aerosolized inactivated vaccine, *Jama.* 207 (1969) 520–524.
796 doi:10.1001/jama.207.3.520.
- 797 [17] J. Tomar, P.A. Born, H.W. Frijlink, W.L.J. Hinrichs, Dry influenza vaccines: towards a stable,
798 effective and convenient alternative to conventional parenteral influenza vaccination,
799 *Expert Review of Vaccines.* 15 (2016) 1431–1447. doi:10.1080/14760584.2016.1182869.
- 800 [18] N. Marasini, L.M. Kaminskis, Subunit-based mucosal vaccine delivery systems for
801 pulmonary delivery - Are they feasible? *Drug Dev Ind Pharm.* 45 (2019) 882–894.
802 doi:10.1080/03639045.2019.1583758.
- 803 [19] T.T. Mutukuri, N.E. Wilson, L.S. Taylor, E.M. Topp, Q.T. Zhou, Effects of drying method and
804 excipient on the structure and physical stability of protein solids: Freeze drying vs. spray
805 freeze drying, *International Journal of Pharmaceutics.* 594 (2021) 120169.
806 doi:10.1016/j.ijpharm.2020.120169.
- 807 [20] H.P. Patil, S. Murugappan, W. ter Veer, T. Meijerhof, A. de Haan, H.W. Frijlink, et al.,
808 Evaluation of monophosphoryl lipid A as adjuvant for pulmonary delivered influenza
809 vaccine, *J Control Release.* 174 (2014) 51–62. doi:10.1016/j.jconrel.2013.11.013.
- 810 [21] C. Thomas, V. Gupta, F. Ahsan, Particle size influences the immune response produced by
811 hepatitis B vaccine formulated in inhalable particles, *Pharmaceutical Research.* 27 (2010)
812 905–919. doi:10.1007/s11095-010-0094-x.
- 813 [22] J.-P. Amorij, V. Saluja, A.H. Petersen, W.L.J. Hinrichs, A. Huckriede, H.W. Frijlink, Pulmonary
814 delivery of an inulin-stabilized influenza subunit vaccine prepared by spray-freeze drying
815 induces systemic, mucosal humoral as well as cell-mediated immune responses in BALB/c
816 mice, *Vaccine.* 25 (2007) 8707–8717. doi:10.1016/j.vaccine.2007.10.035.
- 817 [23] C. Parlati, P. Colombo, F. Buttini, P.M. Young, H. Adi, A.J. Ammit, et al., Pulmonary spray
818 dried powders of tobramycin containing sodium stearate to improve aerosolization
819 efficiency, *Pharmaceutical Research.* 26 (2009) 1084–1092. doi:10.1007/s11095-009-9825-
820 2.
- 821 [24] F. Martinelli, A.G. Balducci, A. Kumar, F. Sonvico, B. Forbes, R. Bettini, et al., Engineered
822 sodium hyaluronate respirable dry powders for pulmonary drug delivery, *International*
823 *Journal of Pharmaceutics.* 517 (2017) 286–295. doi:10.1016/j.ijpharm.2016.12.002.
- 824 [25] J.T. Schiller, M. Müller, Next generation prophylactic human papillomavirus vaccines, *Lancet*
825 *Oncol.* 16 (2015) e217–25. doi:10.1016/S1470-2045(14)71179-9.
- 826 [26] Storage and Handling of GARDASIL®9 (Human Papillomavirus 9-valent Vaccine,
827 Recombinant), <https://www.merckvaccines.com/gardasil9/storage-handling/> (accessed
828 2021, January 31st).
- 829 [27] V. Revaz, R. Zurbriggen, C. Moser, J.T. Schiller, F. Ponci, M. Bobst, et al., Humoral and cellular
830 immune responses to airway immunization of mice with human papillomavirus type 16
831 virus-like particles and mucosal adjuvants, *Antiviral Res.* 76 (2007) 75–85.
832 doi:10.1016/j.antiviral.2007.05.005.
- 833 [28] N.K. Kunda, J. Peabody, L. Zhai, D.N. Price, B. Chackerian, E. Tumban, et al., Evaluation of
834 the thermal stability and the protective efficacy of spray-dried HPV vaccine, *Gardasil® 9,*
835 *Hum Vaccin Immunother.* 15 (2019) 1995–2002. doi:10.1080/21645515.2019.1593727.

Field Code Changed

- 836 [29] S. Saboo, E. Tumban, J. Peabody, D. Wafula, D.S. Peabody, B. Chackerian, et al., Optimized
837 Formulation of a Thermostable Spray-Dried Virus-Like Particle Vaccine against Human
838 Papillomavirus, *Molecular Pharmaceutics*. 13 (2016) 1646–1655. doi:10.1021/acs.molpharmaceut.6b00072.
839
- 840 [30] R.L. Garcea, N.M. Meinerz, M. Dong, H. Funke, S. Ghazvini, T.W. Randolph, Single-
841 administration, thermostable human papillomavirus vaccines prepared with atomic layer
842 deposition technology, *NPJ Vaccines*. 5 (2020) 45–8. doi:10.1038/s41541-020-0195-4.
- 843 [31] E. Canali, A. Bolchi, G. Spagnoli, H. Seitz, I. Rubio, T.A. Pertinhez, et al., A high-performance
844 thioredoxin-based scaffold for peptide immunogen construction: proof-of-concept testing
845 with a human papillomavirus epitope, *Sci Rep*. 4 (2014) 4729. doi:10.1038/srep04729.
- 846 [32] H. Seitz, L. Ribeiro-Müller, E. Canali, A. Bolchi, M. Tommasino, S. Ottonello, et al., Robust In
847 Vitro and In Vivo Neutralization against Multiple High-Risk HPV Types Induced by a
848 Thermostable Thioredoxin-L2 Vaccine, *Cancer Prev Res (Phila)*. 8 (2015) 932–941.
849 doi:10.1158/1940-6207.CAPR-15-0164.
- 850 [33] B. Huber, J.W. Wang, R.B.S. Roden, R. Kirnbauer, RG1-VLP and Other L2-Based, Broad-
851 Spectrum HPV Vaccine Candidates, *J Clin Med*. 10 (2021) 1044. doi:10.3390/jcm10051044.
- 852 [34] I. Rubio, A. Bolchi, N. Moretto, E. Canali, L. Gissmann, M. Tommasino, et al., Potent anti-
853 HPV immune responses induced by tandem repeats of the HPV16 L2 (20 -- 38) peptide
854 displayed on bacterial thioredoxin, *Vaccine*. 27 (2009) 1949–1956.
855 doi:10.1016/j.vaccine.2009.01.102.
- 856 [35] S. Liu, R. Tobias, S. McClure, G. Styba, Q. Shi, G. Jackowski, Removal of endotoxin from
857 recombinant protein preparations, *Clin Biochem*. 30 (1997) 455–463. doi:10.1016/s0009-
858 9120(97)00049-0.
- 859 [36] E. Gasteiger, C. Hoogland, A. Gattiker, S. Duvaud, M.R. Wilkins, R.D. Appel, Protein
860 Identification and Analysis Tools on the ExPASy Server, in: J.M. Walker (Ed.), *The Proteomics
861 Protocols Handbook*, n.d.: pp. 571–607.
- 862 [37] F. Ruscitti, F. Ravanetti, V. Bertani, L. Ragionieri, L. Mecozzi, N. Sverzellati, et al.,
863 Quantification of Lung Fibrosis in IPF-Like Mouse Model and Pharmacological Response to
864 Treatment by Micro-Computed Tomography, *Front Pharmacol*. 11 (2020) 1117.
865 doi:10.3389/fphar.2020.01117.
- 866 [38] P. Sehr, K. Zumbach, M. Pawlita, A generic capture ELISA for recombinant proteins fused to
867 glutathione S-transferase: validation for HPV serology, *J Immunol Methods*. 253 (2001)
868 153–162. doi:10.1016/s0022-1759(01)00376-3.
- 869 [39] I. Rubio, H. Seitz, E. Canali, P. Sehr, A. Bolchi, M. Tommasino, et al., The N-terminal region
870 of the human papillomavirus L2 protein contains overlapping binding sites for neutralizing,
871 cross-neutralizing and non-neutralizing antibodies, *Virology*. 409 (2011) 348–359.
872 doi:10.1016/j.virol.2010.10.017.
- 873 [40] H. Seitz, T. Danthony, F. Burkart, S. Ottonello, M. Müller, Influence of oxidation and
874 multimerization on the immunogenicity of a thioredoxin-l2 prophylactic papillomavirus
875 vaccine, *Clin Vaccine Immunol*. 20 (2013) 1061–1069. doi:10.1128/CVI.00195-13.
- 876 [41] P.M. Day, Y.Y.S. Pang, R.C. Kines, C.D. Thompson, D.R. Lowy, J.T. Schiller, A human
877 papillomavirus (HPV) in vitro neutralization assay that recapitulates the in vitro process of
878 infection provides a sensitive measure of HPV L2 infection-inhibiting antibodies, *Clin
879 Vaccine Immunol*. 19 (2012) 1075–1082. doi:10.1128/CVI.00139-12.
- 880 [42] R.N. Coler, S. Bertholet, M. Moutafsi, J.A. Guderian, H.P. Windish, S.L. Baldwin, et al.,
881 Development and characterization of synthetic glucopyranosyl lipid adjuvant system as a
882 vaccine adjuvant, *PLoS ONE*. 6 (2011) e16333. doi:10.1371/journal.pone.0016333.

- 883 [43] M.A. Arias, G.A. Van Roey, J.S. Tregoning, M. Moutaftsi, R.N. Coler, H.P. Windish, et al.,
884 Glucopyranosyl Lipid Adjuvant (GLA), a Synthetic TLR4 agonist, promotes potent systemic
885 and mucosal responses to intranasal immunization with HIVgp140, PLoS ONE. 7 (2012)
886 e41144. doi:10.1371/journal.pone.0041144.
- 887 [44] N.K. Childers, K.L. Miller, G. Tong, J.C. Llarena, T. Greenway, J.T. Ulrich, et al., Adjuvant
888 activity of monophosphoryl lipid A for nasal and oral immunization with soluble or
889 liposome-associated antigen, *Infect. Immun.* 68 (2000) 5509–5516.
890 doi:10.1128/iai.68.10.5509-5516.2000.
- 891 [45] N.C. Santos, A.C. Silva, M.A.R.B. Castanho, J. Martins-Silva, C. Saldanha, Evaluation of
892 lipopolysaccharide aggregation by light scattering spectroscopy, *Chembiochem.* 4 (2003)
893 96–100. doi:10.1002/cbic.200390020.
- 894 [46] S. Belotti, A. Rossi, P. Colombo, R. Bettini, D. Rekkas, S. Politis, et al., Spray-dried amikacin
895 sulphate powder for inhalation in cystic fibrosis patients: The role of ethanol in particle
896 formation, *Eur J Pharm Biopharm.* 93 (2015) 165–172. doi:10.1016/j.ejpb.2015.03.023.
- 897 [47] R. Vehring, Pharmaceutical particle engineering via spray drying, *Pharmaceutical Research.*
898 25 (2008) 999–1022. doi:10.1007/s11095-007-9475-1.
- 899 [48] G. Spagnoli, A. Bolchi, D. Cavazzini, S. Pouyanfard, M. Müller, S. Ottonello, Secretory
900 production of designed multi-peptides displayed on a thermostable bacterial thioredoxin
901 scaffold in *Pichia pastoris*, *Protein Expr Purif.* 129 (2017) 150–157.
902 doi:10.1016/j.pep.2016.04.012.
- 903 [49] G. Spagnoli, S. Pouyanfard, D. Cavazzini, E. Canali, S. Maggi, M. Tommasino, et al., Broadly
904 neutralizing antiviral responses induced by a single-molecule HPV vaccine based on
905 thermostable thioredoxin-L2 multi-peptide nanoparticles, *Sci Rep.* 7 (2017) 18000.
906 doi:10.1038/s41598-017-18177-1.
- 907 [50] S. Pouyanfard, G. Spagnoli, L. Bulli, K. Balz, F. Yang, C. Odenwald, et al., Minor Capsid Protein
908 L2 Polytope Induces Broad Protection against Oncogenic and Mucosal Human
909 Papillomaviruses, *J Virol.* 92 (2018). doi:10.1128/JVI.01930-17.
- 910

Table 1. Manufacturing parameters and aerodynamic properties of antigen-lacking powders containing different amounts of sodium stearate¹

Powder #	Sodium Stearate (% w/w)	pH of Feed Solution	Yield (%)	D_{v,50}	EF (%)	RF (%)
1	-	5.89	54.63	6.08 (0.74)	87.51 (2.01)	43.52 (4.01)
2	0.33	5.88	31.53	18.58 (2.44)	75.16 (5.17)	8.02 (3.04)
3	1.00	7.94	43.72	3.40 (0.73)	89.89 (1.32)	48.10 (9.39)
4	2.00	8.14	59.46	26.35 (3.09)	94.46 (2.69)	13.59 (7.21)

¹Sodium stearate content (as percentage by weight of the solutes contained in the feed solution), production yield, pH of the feed solutions, median volume diameter (D_{v,50}), Emitted Fraction (EF, as percentage of the loaded amount) and Respirable Fraction (RF, as percentage of the loaded amount) of powders prepared with different amounts of sodium stearate. Mean values and standard deviations in parenthesis (n=3).

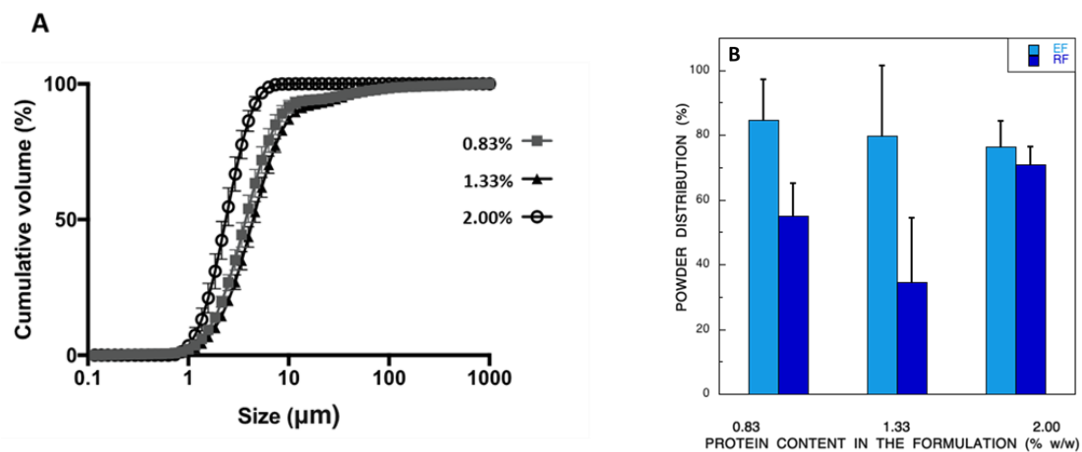


Figure 1. (A) Particle cumulative undersize distribution evaluated by laser light diffraction of spray-dried powders 3a, #3b and #3c containing different amounts of the antigen: 0.83% w/w (*squares*), 1.33% w/w (*triangles*), 2.00% w/w (*empty circles*) (mean values and standard deviation bars are indicated; n=3). **(B)** Emitted fraction (EF) and Respirable Fraction (RF) aerodynamic properties of three powders containing different amounts of the *PfTrx-HPV-L2* antigen as indicated. Mean and standard deviation values (n=3) are indicated.

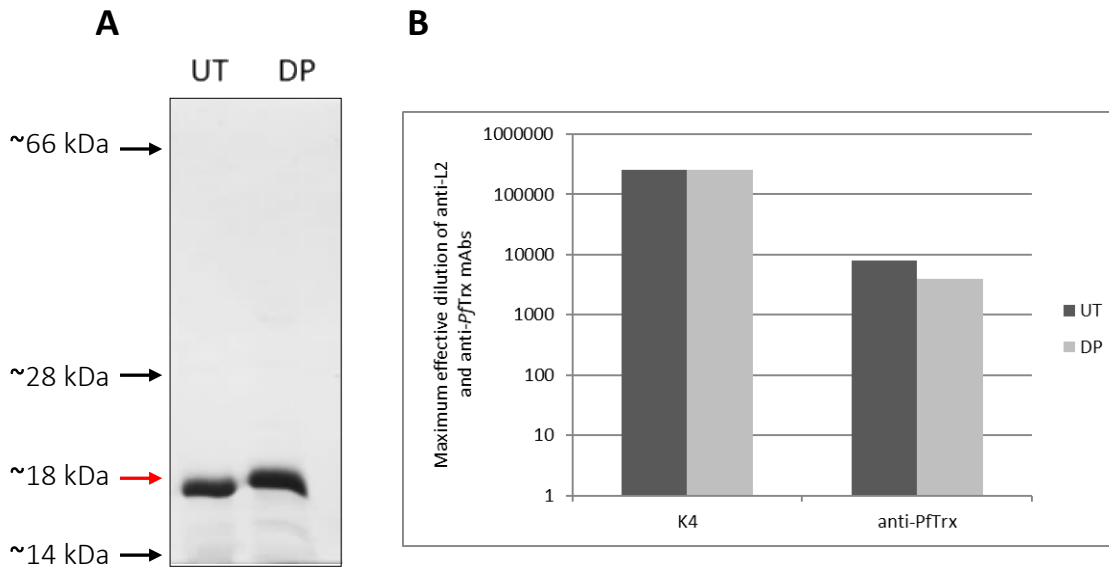


Figure 2. (A) SDS-PAGE analysis of the untreated (UT) liquid-form and the dry-powder formulated (DP) *PfTrx*-HPV-L2 antigen. The expected migration position of the *PfTrx*-HPV-L2 protein is indicated by a red arrow; the migration positions of molecular mass markers are indicated by black arrows. **(B)** Comparative ELISA analysis of the immunoreactivity of the untreated (UT, dark-grey) and the dry-powder formulated (DP, light-grey) *PfTrx*-HPV-L2 antigen. mAbs directed against the L2 epitope (K4) or the *Pyrococcus* thioredoxin scaffold (anti-*PfTrx*) were used as primary antibodies. The results are the average of two technical replicates, which differed by no more than 5% of the mean.

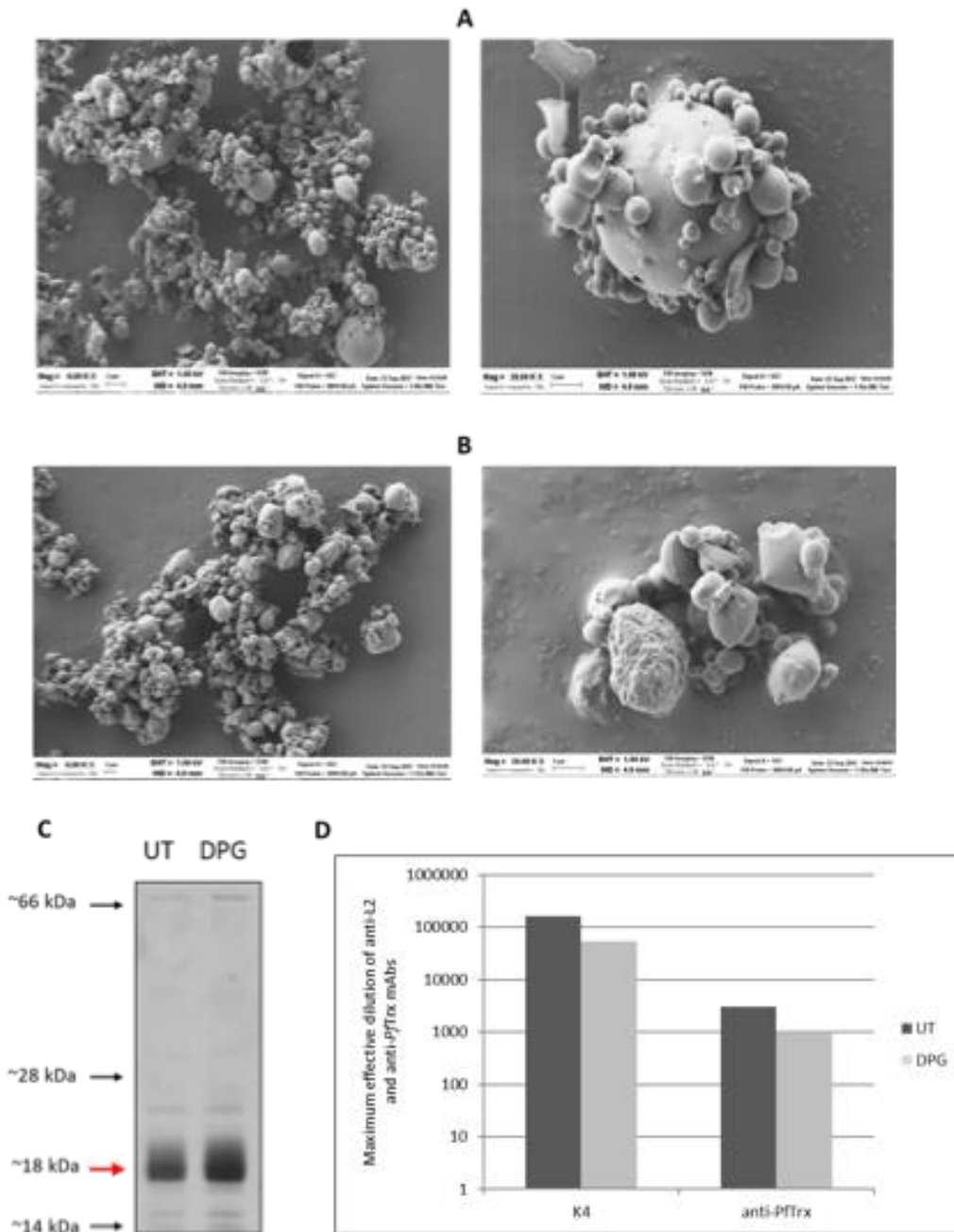


Figure 3. SEM images of the GLA-containing powder #5 (1.33% w/w of *PfTrx*-HPV-L2) (**A**) and powder #6 containing 2.00% w/w *PfTrx*-HPV-L2 (**B**). Magnification 6.000x (left-hand image) and 20.000x (right-hand image). (**C**) SDS-PAGE analysis of the untreated liquid-form (UT) and the dry-powder-GLA formulated (DPG) *PfTrx*-HPV-L2 antigen. The expected migration position of the *PfTrx*-HPV-L2 protein is indicated by a red arrow; the migration positions of molecular mass markers are indicated by black arrows. (**D**) ELISA analysis of the untreated (UT, dark-grey) and the dry-powder-GLA formulated (DPG, light-grey) *PfTrx*-HPV-L2 antigen. mAbs directed against the L2 epitope (K4) or the *Pyrococcus* thioredoxin scaffold (anti-*PfTrx*) were used as primary antibodies for detection. The results are the average of two technical replicates, which differed by no more than 5% of the mean.

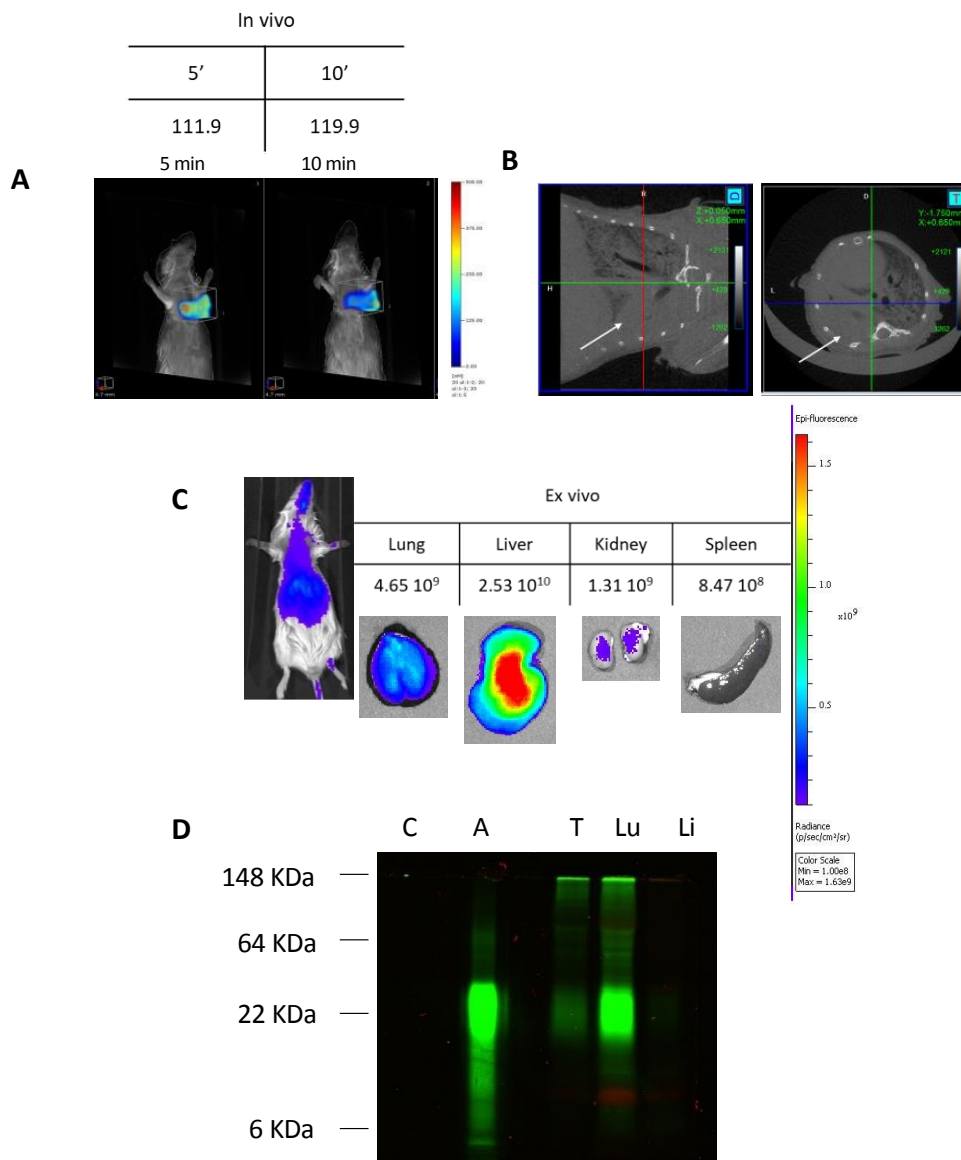


Figure 4. Tissue distribution of the Alexa Fluor750-labeled *PfTrx*-HPV-L2 antigen delivered intratracheally in liquid form. Intratracheally administered, pre-dissolved Alexa-labeled vaccine powder visualized by FMT, 5 and 10 min after intratracheal delivery (**A**) and by Micro-CT (**B**) imaging (transversal and coronal views are shown in the left- and right-side images, respectively, where the arrows indicate the accumulation sites of the delivered liquid vaccine). *In vivo* (**C**, left-side panel) and *ex-vivo* multi-organ (**C**, right-side panel) IVIS imaging of the Alexa-labeled *PfTrx*-HPV-L2 antigen 15 min after intratracheal administration. (**D**) SDS-PAGE fractionation and fluorescence-based visualization of trachea (T), lung (Lu) and liver (Li) tissue homogenates derived from a mouse, to which the pre-dissolved, Alexa-labeled dry-powder vaccine was administered intratracheally; equivalent amounts (5 ng) of the unlabeled (C) and the Alexa-labeled (A) *PfTrx*-HPV-L2 protein served as controls for this experiment. The results are from a representative experiment that was performed in parallel on two different animals.

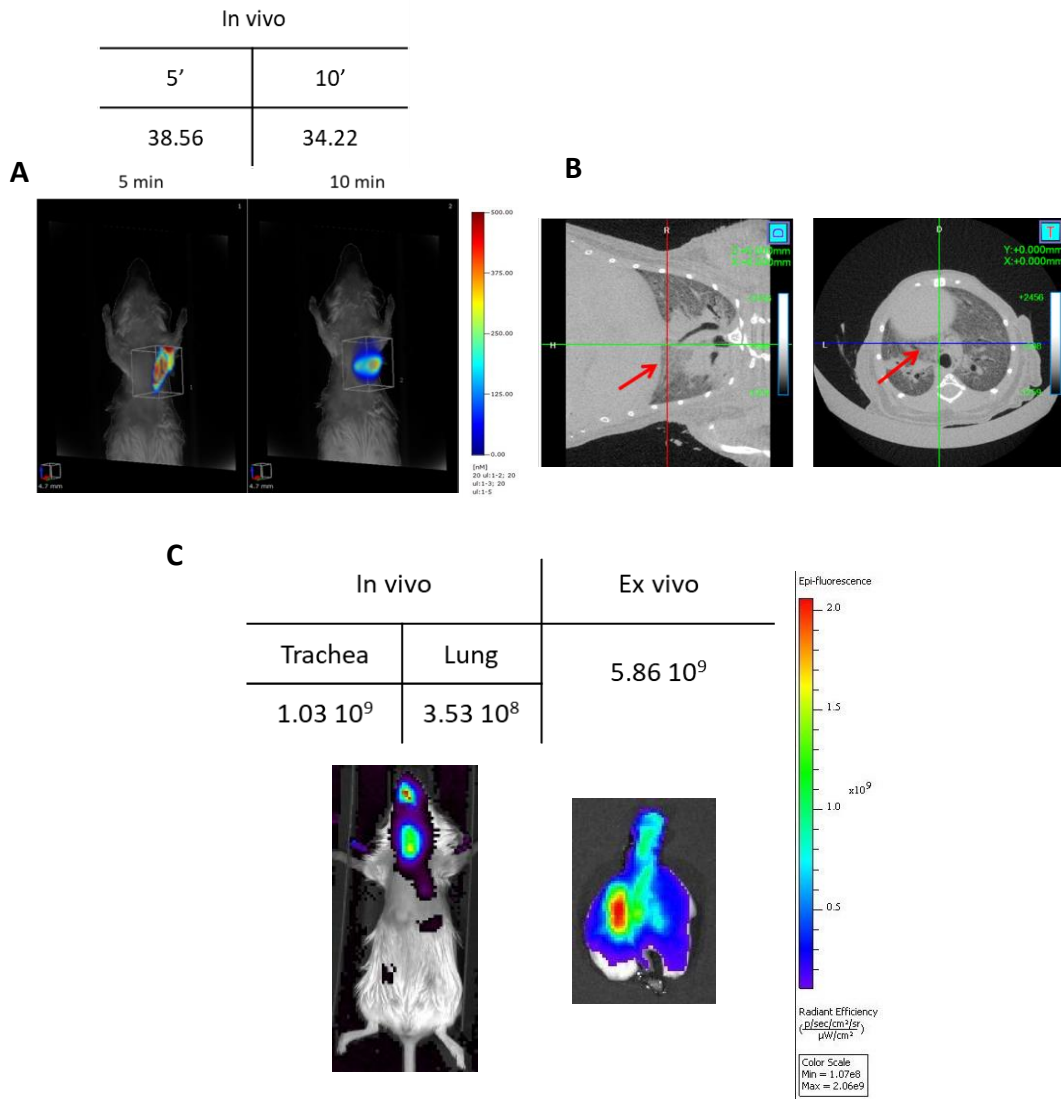


Figure 5. Lung deposition of the intratracheally administered dry-powder vaccine. (A) *In vivo* total body FMT imaging of the Alexa Fluor750-labelled *Pf*Trx-HPV-L2 antigen distribution at two different time-points (5 and 10 min) after administration of the vaccine powder. (B) Micro-CT imaging of antigen deposition into the lungs; transversal and coronal views are shown in the left- and right-side images, respectively, where the arrows indicate the vaccine powder deposition sites. (C) *In vivo* (left panel) and *ex-vivo* (right panel), IVIS analysis of Alexa Fluor 750-labelled *Pf*Trx-HPV-L2 accumulation in the respiratory tract, 15 min after intratracheal delivery of the dry-powder vaccine.

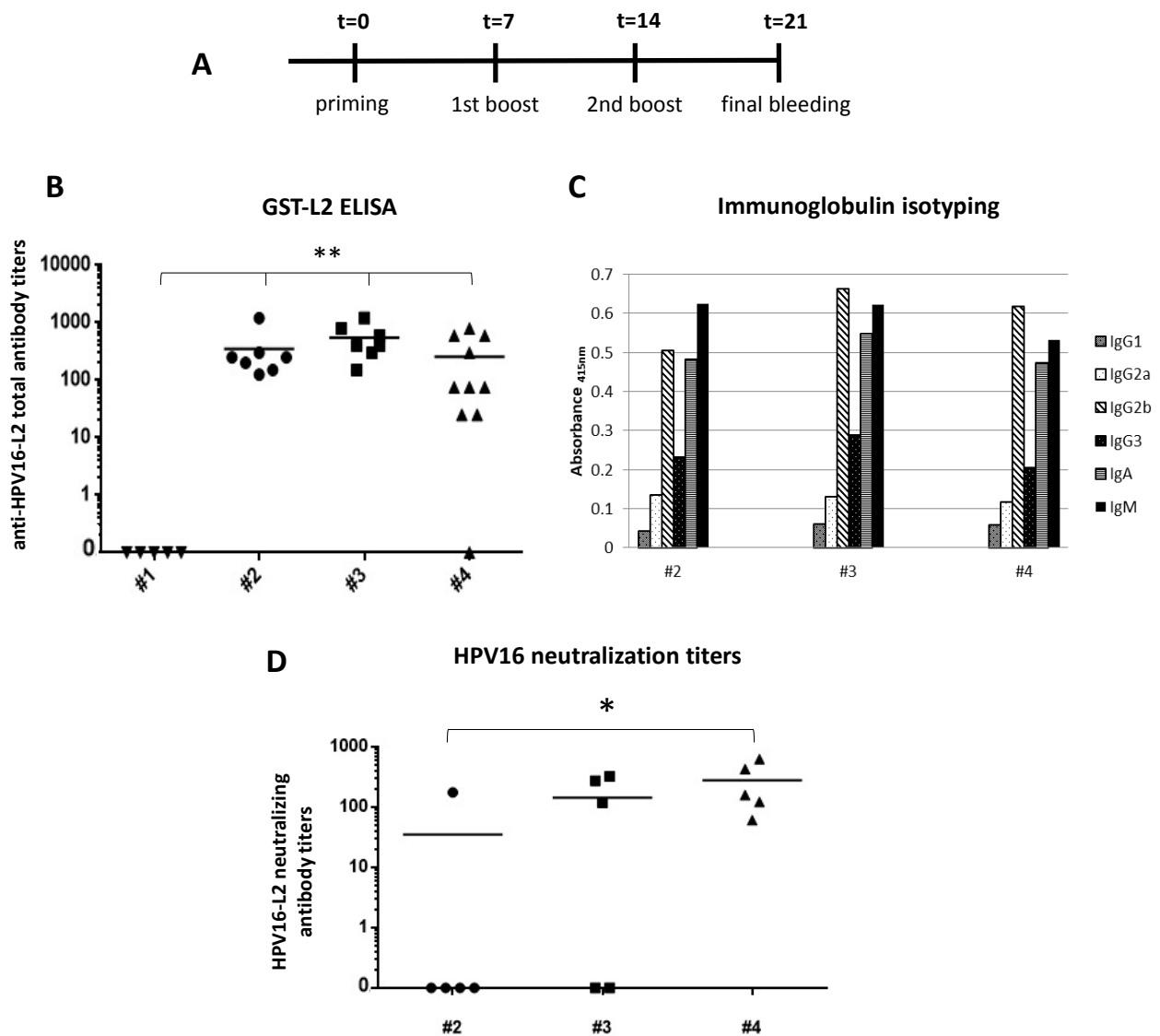
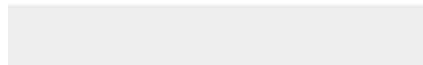


Figure 6. Immunogenicity profiling. **(A)** Timeline of the short-term immunization experiment performed with the GLA-adjuvanted, *PfTrx*-HPV-L2 DPI delivered intratracheally. **(B)** GST-L2 ELISA performed on sera from differently treated groups of mice, collected one week after the last immunization. The following treatments were applied to individual groups: #1, negative control, subcutaneous immunization with solubilized, GLA only containing powder with no antigen; #2, subcutaneously injected, liquid form, GLA+alum adjuvanted *PfTrx*-HPV-L2 antigen; #3 subcutaneously injected *PfTrx*-HPV-L2-[GLA] dry-powder vaccine solubilized in PBS immediately before administration; #4, *PfTrx*-HPV-L2-[GLA] dry-powder vaccine administered intratracheally. Data represent anti-HPV-L2 total antibody titers measured in individual mice; the means of the titers for each group are indicated by horizontal lines (** $p \leq 0.01$). **(C)** Immunoglobulin isotyping of pooled sera from the mice groups (#2, #3 and #4) shown in panel B, except for the completely unresponsive, negative control group #1. **(D)** HPV16 neutralization titers determined by the L2-PBNA on a subset of five immune-sera/group (#2, #3 and #4) derived from the animals in each group that displayed the highest (top five) anti-HPV-L2 total antibody titers by GST-L2 ELISA (panel B). Data represent neutralizing antibody titers measured in individual mice; mean values of the titers for each group are indicated by horizontal lines (* $p \leq 0.05$).



Click here to access/download
Supplementary Material
Supplementary Material-Rev.docx



Credit author statment

Irene Rossi, and **Gloria Spagnoli**, Investigation, Writing original draft; **Fabio Stellari** and **Quigxin Chen**: investigation; **Francesca Buttini** and **Fabio Sonvico**: Validation, Methodology; **Davide Cavazzini** and **Angelo Bolchi**: Resources, Data curation; **Martin Müller**: Formal analysis; **Simone Ottonello** and **Ruggero Bettini**: Conceptualization, Writing Reviewing and Editing, Funding aquisition